Design of a Race Car Differential

Stefan Kloppenborg

A thesis submitted in partial fulfillment
of the requirements for the degree of

BACHELOR OF APPLIED SCIENCE

Supervisor: Prof. W.L. Cleghorn

Department of Mechanical and Industrial Engineering
University of Toronto

March 2008

Abstract

In a race car, the differential plays two important roles which contribute to the overall performance of the vehicle. First, the differential splits the torque from the engine to the two driven wheels to produce longitudinal acceleration. The characteristics of the differential will dictate the maximum attainable longitudinal acceleration under certain conditions, such as when exiting a corner. The differential will also impart a yaw moment to the vehicle when turning which will tend to either turn the car into the turn, or resist the turn. This is an often overlooked effect of the differential, but can have a significant effect on the handling of the car. The characteristics of the differential will dictate the yaw moment produced. This effect has been studied with vehicle dynamics models, as well as on-track testing. The results of both show the the differential characteristics that allow the maximum longitudinal acceleration also produces a yaw moment resisting turning at low levels of acceleration, and an oversteer yaw moment at high acceleration, making the car more difficult to drive. The relative importance of these two effects is dependent on the track being driven. Tracks with lots of sharp corners favor a low-lock differential, while tracks with fast, large radius corners favor high-lock differentials.

In order to study the effect of the differential on an actual vehicle, an adjustable salisbury differential was designed and built for the University of Toronto Formula SAE car. This differential is unique in the fact that it's clutch pack can be adjusted without disassembling the unit. Adjustments can be made in about two minutes, and it has been found that these adjustments have a large effect on the handling of the car. The mechanical design of this differential has used techniques such as CAD, FEA hand calculations and physical testing. Three iterations of this differential have been designed, and two have been built and tested. While there have been reliability issues, the design is converging to a reliable one.

Acknowledgments

A number of people and companies have aided in the design, construction and testing of the differential described in this thesis. Much of the work would not have been possible without their help.

The University of Toronto Formula SAE (FSAE) team has provided has made this project possible. The differentials have been tested on U of T FSAE cars, the team has financed the project and the team members have aided in the construction. In particular, David Boom and Daniel Veneziano have been a huge help, devoting much time to manufacturing the various versions of the differential, as well as providing some design input. Steven Choi aided this project by performing material analysis which was indispensable in benchmarking commercial gears.

The American Gear Manufacturer's Association (AGMA) has also helped this project by providing a copy of the bevel gear design standard, AGMA B97, free of charge. True Gear and Spline, located in Cambridge, has provided gear cutting services at a reduced cost for this project and Precision Gears, located in Brampton, have manufactured many of the part which mate to the differential free of charge. Profile Waterjet, located in London, has provided water jet cutting of the clutch plates and Phoenix Friction Products donated the friction lining for the clutch plates of the first revision of the differential.

Contents

Table of Variables

A	slope of T_c-T line
a	addendum
AS	axle slip
B	preload torque
C	ramp coefficient of differential ($\frac{\partial T_c^{max}}{\partial T_{app}}$)
C_E	elasticity coefficient for hertz formula
C_m	mean pitch cone radius
C_x	longitudinal force coefficient of a tire
D	diameter
D_p	pitch diameter of a gear
DP	diametral pitch
F_{pre}	clutch preload force
F_s	separating force for a gear pair
F_x	longitudinal force of a tire
F_z	vertical force on a tire

ΔF_z	weight transfer
I	contact stress geometry factor
J	bending stress geometry factor
N	yaw moment
N	number of teeth on a gear
N_c	number of clutch plates
N_g	number of teeth on side gear
N_s	number of teeth on spyder gear
p	load per unit length for hertzian contact
P_d	pitch diameter of a gear
R	turn radius
R_t	tire radius
r	yaw rate
r_c	mean radius of clutch plates
r_r	distance from center of differential to ramp
s	dedendum
T_{app}	torque applied to differential
T_c	locking torque of differential
T_c^{max}	torque required to overcome clutch friction
T_g	torque seen by differential gear set
T_l	torque applied to left wheel
T_r	torque applied to right wheel
T_s	torque on spyder gear

ΔT	difference between left and right axle torque ($\lvert T_l - T_r \rvert$)
t	track
V	velocity
V_l	road speed under left wheel
V_r	road speed under right wheel
X	longitudinal force
Y	lateral force
α	slip angle
α	ramp angle in a salisbury differential
β	body slip angle
δ	steering angle
ϕ	contact angle
κ	slip ratio
μ_c	coefficient of friction of clutch plates
Ω	driven axle rotational speed
ω_{app}	rotational speed of differential housing
Ω_d	difference in left and right wheel speed
Ω_l	left wheel rotational speed
Ω_r	right wheel rotational speed
σ	stress

List of Figures

List of Tables

Chapter 1

Introduction and Background

1.1 Aim of Current Research

A differential is an important part of a race car that can have a large effect on the car's performance. It serves two primary purposes. The differential determines how much torque is distributed to each of the two driven wheels. This distribution determines the maximum amount of in-line acceleration possible and also imparts a yaw moment to the car which affects the handling. In designing a differential for a race car, both of these effects must be carefully considered. The following document outlines the design of a differential for the University of Toronto Formula SAE car. This differential was designed to be adjustable to allow for tuning of the two aforementioned effects. In order to gain a better understanding of the effect of the parameters of the differential on the performance of a car, vehicle dynamic simulation and track testing is performed.

1.2 Function of a Differential

Since a car has its drive wheels a finite lateral distance apart, when negotiating a corner, the drive wheels must turn at different rates. Let's call the distance from the center of the turn to the centerline of the car R, and the track (distance between the left and right wheels) t. The inside wheel is running on a circle of radius $R - \frac{t}{2}$, while the outside wheel is running on a circle of radius $R + \frac{t}{2}$. The yaw rate, r, of the vehicle in a steady-turn will be how much of the circle the vehicle negotiates in a unit of time (usually expressed in $rad \cdot s^{-1}$). If the tire radius is called R_t, then the inside wheel will turn at a rate of $\Omega_i = \frac{R - \frac{t}{2}r}{R_t}$ while the outside wheel will turn at a rate of $\Omega_o = \frac{(R + \frac{t}{2})r}{R_t}$. Thus, the difference in driven wheel speed will be $\Omega_d = \frac{tr}{R_t}$.

The most basic type of differential is called an open differential. This is the type of differential found in most road cars. It has the property that it splits the input torque equally between the two driven wheels. Introducing the notation for right and left wheel torque, an open differential has the following property:

$$T_r = T_l \tag{1.1}$$

An open differential has the additional property that it will allow completely free differentiation. The wheel speeds will be whatever they need to be in order to satisfy Eq (1.1). If one wheel has considerably less tractive capacity than the other, this property becomes a problem. Since the wheel torque must be equal left and right, the wheel with higher tractive capacity cannot utilize it because it is limited by the lower traction wheel. Such a situation occurs in a road car when one wheel is on dry pavement and the other on ice. This is even more of a problem in a racing car where high lateral accelerations are experienced. The inside wheel will have considerably less vertical load on it than the outside wheel (due to weight transfer caused by having a CG above the ground). The less loaded wheel cannot transmit as much force because the friction with the road is overcome more easily. To reduce this negative effect, limited slip differentials have been developed.

A limited slip differential (LSD) will resist a difference in wheel speed. A common way of doing this is to connect the two driven wheels together with a clutch. Defining the torque that resists differentiation as T_c, the general expression for left and right wheel torque becomes:

$$T_r - T_l \leq sgn\,(\Omega_l - \Omega_r)\,T_c \tag{1.2}$$

Where sgn is the sign operator. It has a value of $+1$ when the argument is positive and has a value of -1 when the argument is negative.

Eq (1.2) applies for all types of LSDs. What sets the various types of differentials apart is the function governing T_c.

1.3 Types of Differentials

Many types of limited slip differentials have been developed over the years. The most common are:

1. Passive clutch pack
2. Salisbury
3. Torsen
4. Viscous coupling
5. Cam and pawl
6. Detroit locker

As noted earlier, the main feature that sets these types of LSDs apart is T_c and how it varies. In a passive clutch pack differential, T_c is generated by two clutch plates being pressed together with a set of springs. The spring force is constant, and hence, T_c is constant.

A Salisbury differential increases T_c with increased applied drive torque. Thus, a salisbury differential can be made to be almost open (no resistance to differentiation) when no drive torque is applied and nearly locked when drive torque is applied. A Torsen differential has the same characteristics. The only difference is the manner in which T_c is generated. A Torsen uses the friction in a helical gear mesh to generate T_c, while a salisbury differential uses a clutch pack. For a full discussion of the operation of a Torsen differential, see [3].

A viscous coupling generates T_c based on the relative speed of the two drive wheels. The value of T_c is approximately proportional to the difference in driven wheel speed. A detroit locker is another speed sensing differential. The T_c for a detroit locker is related to the difference in driven wheel speed, but not linearly as in a viscous coupling; a detroit locker can only be fully open or fully locked [4]. A cam and pawl differential is another speed-sensing differential, but is much more progressive than the detroit locker [4].

It is worth briefly mentioning two other types of differentials: the spool and the active differential. The former is not actually a differential, but is usually discussed in the same context. A spool is a device that does not allow differentiation. The simplest incarnation would be simply connecting the driven wheels together with a single shaft so that they are constrained to turn at the same rate. As will be seen, a salisbury differential can act as a spool under certain conditions. Under these conditions, its effect on the handling of the car will be identical to that of a spool. An active differential is conceptually similar to all LSDs, except that the value for T_c is chosen by a computer. This computer can used any number of variables to choose the appropriate level of T_c.

1.4 Choice of the type of differential

The choice of the type of differential to develop for this investigation was a critical one. First, the speed-sensing differentials were ruled out because they are inherently reactive devices. In order for them to achieve any level of T_c, one wheel must be spinning significantly faster than the other. If one wheel has already started spinning to an extent that a viscous coupling will start to resist differentiation, it's too late: the tire has already lost much its longitudinal and lateral force capacity. A torque sensing differential like a Salisbury or Torsen has the advantage that the T_c is available before it is required. While a Torsen is a marvelous mechanical system, the only way that the characteristics of the differential can be changed is by adjusting the helix angles of the gears [3]. This rules out making a adjustable Torsen differential. This leaves only two options for a differential suitable for studying the effects of a differential on vehicle dynamics: a Salisbury or an active differential. An active differential was investigated, but preliminary calculations indicated that the weight of the unit would be many times greater than that of a Salisbury unit, and the current drain on the car's electrical system would be quite high. Thus, a Salisbury type differential was chosen, and designed such that the clutch pack could be easily adjusted.

1.5 Mechanical Iterations

In order to study the effect of the differential on track, a differential with an adjustable clutch was designed and built (see chapter 2 for a description of what the clutch does and why it's important). To date, three versions have been designed. The first two versions, the Mk I and the Mk II, have been build and tested; the third version, the Mk III, is currently being constructed. Each new version represents a refinement of the previous version. In all cases, the goal of the mechanical design was to minimize the weight of the unit while assuring mechanical reliability throughout a testing season of approximately four months.

1.6 Vehicle Dynamics Background

Vehicle dynamics is the study of how a car responds to driver input. It is a key aspect of the design of both road and racing cars. If a road car is difficult to control – either because the response to driver input insufficient or because the car is unstable – the average person will not be able to drive it safely. In the case of a racing car, vehicle dynamics has become an exacting science. The difference between the podium and the back of the field can be a very small difference in the dynamics of the car.

The tires are the only part of a car that generate lateral and longitudinal force (aerodynamic devices can generate these forces but will not be considered here).

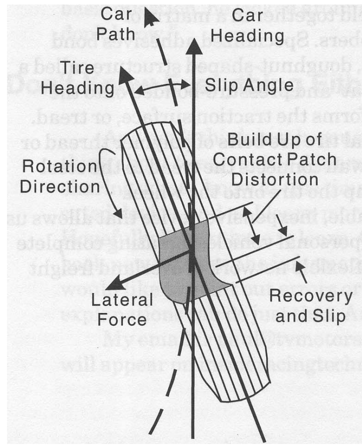

Figure 1.1: Definition of slip angle. Taken from [1]

First, we will look at pure lateral force generation. The way that tires generate lateral force is through a deformation of the tire tread. The quantity *slip angle*, α, is used to quantify the extent of this deformation and used to determine the resulting force. Figure 1.1 shows the definition of slip angle. It is the angle between the direction that the wheel is pointing (labeled "tire heading") and the direction that the wheel is moving (labeled "car heading").

A tire model can be used to determine the lateral force based on the slip angle and the vertical load. Example tire data is shown in figure 1.2. Note that at low value of slip angle, the curves are nearly linear. Basic vehicle dynamics models are often linearized by taking the tire force to be proportional to the slip angle.

Longitudinal tire force, like lateral force, is generated through tire deformation. In the case of longitudinal force, the deformation is measured with the slip ratio, κ. This is the ratio of the actual rotational speed of the tire to

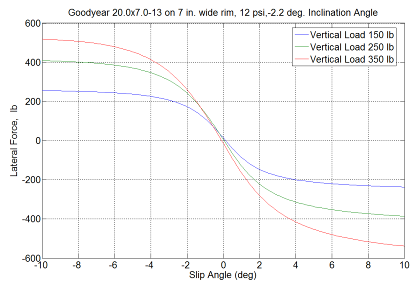

Figure 1.2: Example tire data for pure lateral force generation. Data obtained through the Formula SAE Tire Test Consortium with the aid of Calspan Tire Research Facility (TIRF).

the rotational speed of an undeformed tire. Several mathematical definitions of slip ratio have been proposed. The SAE definition will be used here and is shown in Eq 1.3 [5]. The shape of the longitudinal force vs. slip ratio curves is very similar to the lateral force vs. slip angle curves. Again, models are often linearized by taking the tangent of the curve near the origin.

$$\kappa = \frac{\Omega R_t}{V} - 1 \tag{1.3}$$

Another important quantity in describing the behavior of an entire car rather than just a tire is *body slip angle*, denoted as β. This is the angle between the car's longitudinal axis and the tangent to its path, measured at the center of gravity of the vehicle. This is illustrated in figure 1.3. Also shown in this figure is steering angle, δ. This is the angle that the front wheels make with the center line of the car.

Aeronautical engineers pioneered the use of stability and control derivatives to investigate the performance of an airplane [6]. This technique has

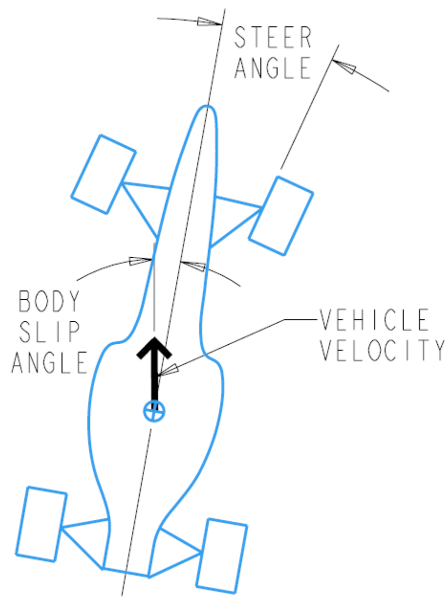

Figure 1.3: Illustration of body slip angle, β, and steering angle, δ.

been extended to cars [7] and can give an engineer a good understanding of how a vehicle will act. This technique begins by finding the equations of motion of the vehicle. In classical cases, the equation for lateral force, Y, and yaw moment, N are found. This concept will be extended to include longitudinal acceleration, X.

Once these equations of motion are found, the partial derivatives with respect to the control variable, steering input, to yield the control derivatives. These partial derivatives indicate how the vehicle will respond to driver input. The stability derivatives are found by differentiating the equations of motion with respect to the state of the vehicle (yaw rate and body slip). These indicate how stable the vehicle is.

Small disturbance theory can be used to investigate the response of the vehicle at small deviations from some initial condition. The stability and control derivatives are evaluated at this initial conditions (denoted as x_0 in Eq 1.4) and the response if found by using Eq 1.4.

$$N = N|_{x=x_0} + N_\beta|_{x=x_0} \Delta\beta + N_r|_{x=x_0} \Delta r + N_\delta|_{x=x_0} \Delta\delta \tag{1.4}$$

Note that for brevity, partial derivative notation in the form of N_r will be introduced. N_r is equivalent to $\frac{\partial N}{\partial r}$.

This can be simplified considerably if the initial condition chosen is one of trim (the sum of all the forces and moment are zero). For example, a model of yaw moment linearized at trim can be written as Eq 1.5. The point that the partial derivatives are evaluated at have been dropped from the notation and are understood to be evaluated at a condition of trim.

$$N = \left(\frac{\partial N}{\partial \beta}\right)\beta + \left(\frac{\partial N}{\partial r}\right) r + \left(\frac{\partial N}{\partial \delta}\right)\delta \tag{1.5}$$

The most important stability derivative is the yaw damping term, $\frac{\partial N}{\partial r}$. This term determines the car's resistance to spinning. If this were to have a positive value, the car would be unstable. An positive value of yaw rate, r, would cause a positive yaw moment, N, which would in turn increase the yaw rate. In almost ever case, this term is negative so this term serves to stabilize the car.

Chapter 2

System Overview

2.1 Overall Layout

A Salisbury differential consists of five basic components: the housing, the gear set, the ramp, the clutch pack and the preload spring(s). The basic layout of a Salisbury differential is show in figure 2.1. The bevel gears that make up the gear set have the same layout as in an open differential. (See [8] for a discussion of open differentials.) A crucial difference between an open differential and a salisbury differential is how the spyder gears (see figure 2.3) are attached to the housing. In an open differential, the shaft passing through the center of both spyder gears is affixed to the housing. This affixed shaft drives the spyder gears. In a salisbury differential, however, the spyder gears are not directly attached to the housing. The ramp is fixed in rotation relative to the housing, but allowed to move along the axis of the differential.

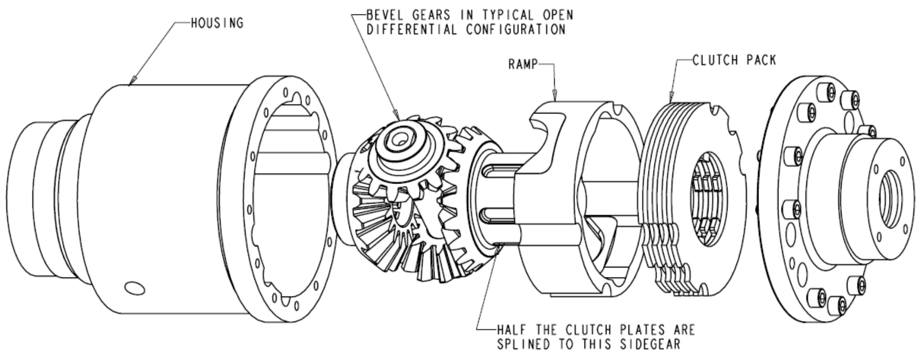

Figure 2.1: Typical layout of a Salisbury differential. Preload spring omitted for clarity

The torque applied to the housing is transmitted to the ramp. The ramp "pushes" on the spyder gear. Since the face of the ramp is angled, it is thrust outwards (see figure 2.2). This, in turn applies normal load to the clutch pack, causing it to increase its resistance to slipping. Half of the clutch plates are splined to one of the side gears while the other clutch plates are splined to the housing. When the unit differentiates, the side gear turns with respect to the housing. The clutch pack resists this rotation. The force on the clutch pack is dependent on the torque applied to the housing according. Typically, springs are also installed in the differential to preload the clutch pack.

2.2 Open Differential

The gear set of a salisbury differential operates just as the gears in an open differential. Two side gears oppose each other – one connected to each half shaft – and two (or sometimes four) spyder gears mesh with these side gears.

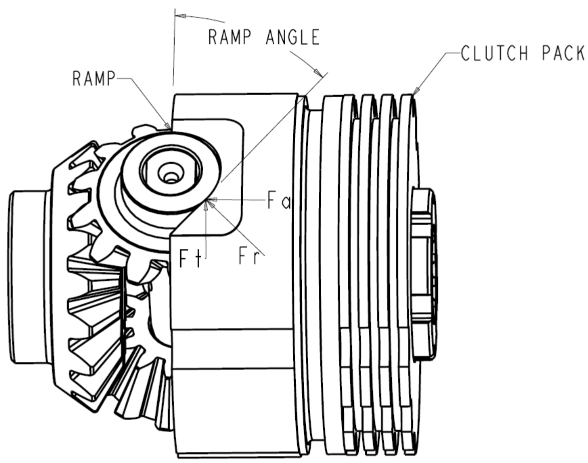

Figure 2.2: Forces on the ramp in a Salisbury differential.

See figure 2.3 for a graphical description.

A differential has a degree of freedom of 2 [8]. This means that there are two distinct motions that can be superimposed. The first motion is the whole differential rotating about the axes of the two side gears. None of the gears rotate relative to one another in this mode of motion. Referring to figure 2.4, $\Omega_{app} = \Omega_l = \Omega_r$. The section type of motion is differentiation. In this mode, the spyder gear carrier remains fixed while the gears rotate relative to one another. If the left side gear is rotating at a rate of Ω_l, the the spyder gear will rotate at a rate of $\Omega_l N_g/N_s$. The right side gear will then rotate at a rate of $-\Omega_l\,(N_g/N_s)\,(N_s/N_g) = -\Omega_l$. The speeds of the gears in the two modes superimposed can be written as Eq 2.1. Note that this equation has one free parameter. In the case of an automotive differential, this parameter ends up being set by the interactions between the tire and the road.

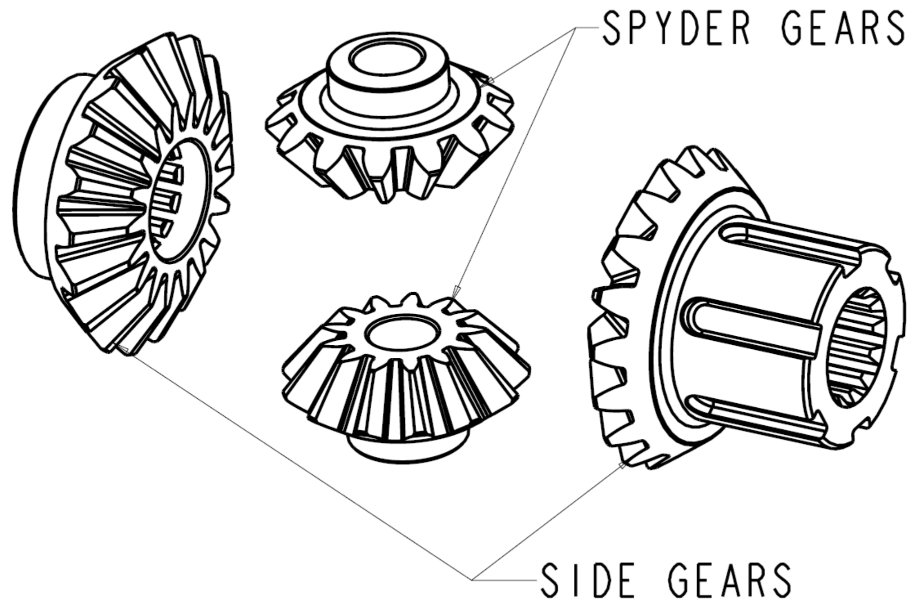

Figure 2.3: Layout of differential gears

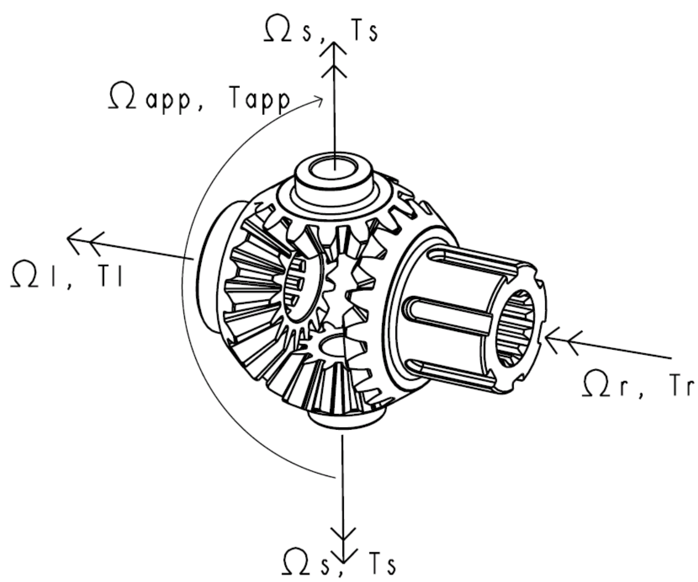

Figure 2.4: Speed of each gear in a differential

$$\Omega_{app} = \frac{\Omega_l + \Omega_r}{2} \tag{2.1}$$

When the torque on each of the components of an open differential is analyzed, the important observation is that the left and right side-gear torque is always the same. This can be seen by taking a force balance on a spyder gear. A force is applied in the center by the carrier. This force is reacted by the two meshes with the side gears. Since the two meshes both occur on the pitch cone of the spyder gear, they act on the same moment arm. Therefore, for the moments to balance on the spyder gear, the force applied to each side gear must be equal. Since the two side gears are of equal diameter, the torque applied to each is equal.

2.3 Torque Path

In the case of a salisbury differential, the torque applied to the differential housing, T_{app}, is reacted by two components of the differential: the gear set and the clutch pack. These torques will be called T_g and T_c respectively. When a given torque is applied to a differential (without a clutch), the right and left output torque (of the gears), T_r and T_l, will be equal. When a clutch is added, torque will effectively be transfered from one side of the differential to the other. The two equations governing this are given as Eq 2.2 and Eq 2.3. The derivations of these expressions are given in appendix B.

$$|\Delta T| = |T_r - T_l| = T_c \tag{2.2}$$

$$T_{app} = T_g + T_c = T_l + T_r \tag{2.3}$$

2.3.1 Clutch Torque

The clutch pack generates a friction couple based on the normal force applied to it. This normal force is generated by both the preload spring and the effect of the pinion being forced against the ramp. An approximate relationship between the various parameters of the differential, the applied torque and the maximum friction torque available from the clutch pack is given as Eq 2.4. This expression is derived in appendix A.

$$T_c^{max} = \frac{C_A T_{app} + N_c r_c \mu_c F_{pre}}{1 + C_A} \tag{2.4}$$

Where

$$C_A = \frac{N_c r_c \mu_c}{r_r \tan \alpha} \tag{2.5}$$

See Appendix A for the definitions of the variables used. This expression can be simplified by defining two variables, C and B which define the slope of the T_c^{max}-T_{app} line and the offset from the origin respectively. Since the coefficient C is controlled by the ramp, it will be called the ramp coefficient.

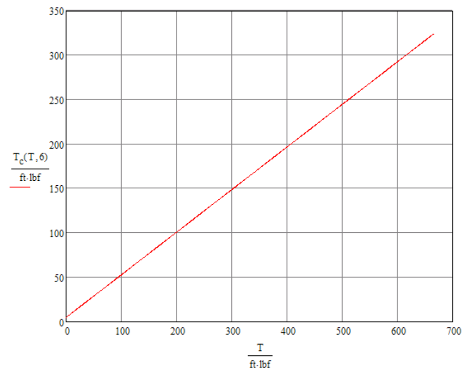

Figure 2.5: Plot of T_c^{max} versus applied torque, T for the Mk II differential. Note the small offset indicating a small preload

	Setting 1		Setting 2		Setting 3	
	C	B	C	B	C	B
Mk I	0.251	$9.62ft \cdot lb$	0.501	$20.2ft \cdot lb$	0.626	$25.2ft \cdot lb$
Mk II	0.316	$1.81ft \cdot lb$	0.480	$2.75ft \cdot lb$	0.581	$3.32ft \cdot lb$
Mk III	0.323	$1.85ft \cdot lb$	0.489	$2.80ft \cdot lb$	0.589	$3.37ft \cdot lb$

Table 2.1: Clutch parameters for the three versions of the U of T differential

B will generally be referred to as the preload. Therefore:

$$T_c^{max} = CT_{app} + B \tag{2.6}$$

The clutch torque, T_c^{max} for the University of Toronto FSAE differential is shown in figure 2.5. The U of T differential has adjustment built into it (see section 2.4), so has different values of C and B depending on the setting. these values are given in table 2.1. For all three versions of the differential, preload has been kept low.

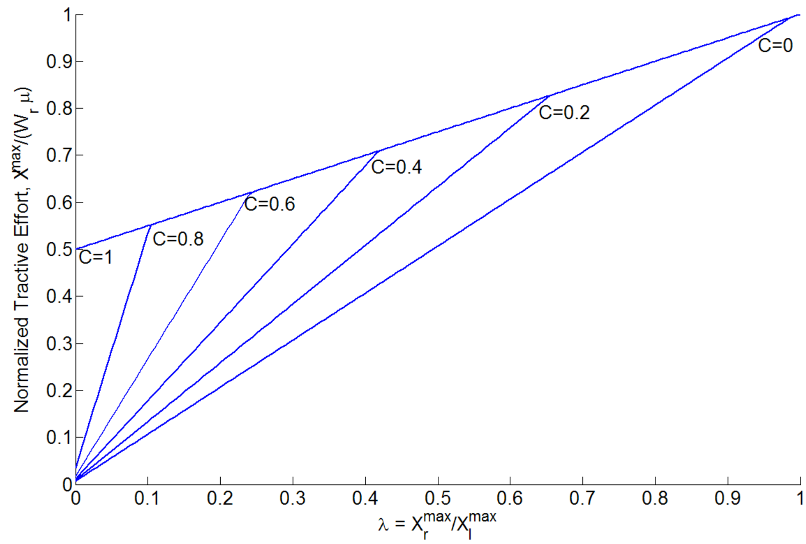

Figure 2.6: Tractive effort for various clutch configurations ($B = 2.85 ft \cdot lb$)

2.3.2 Effect of Clutch Torque on Maximum Tractive Effort

In the case of different vertical load on the two driven tires or the case of a split coefficient surface[1], the left and right tire reach their traction limits with different amounts of torque application. The difference between left and right wheel torque is limited by the differential clutch characteristics, so the maximum tractive effort is a function of both the surface coefficient for the two tires and the clutch characteristics.

Figure 2.6 shows the maximum tractive effort for a split coefficient condi-

[1]A split coefficient surface is a roadway with different coefficients of friction for the right and left tires. An example of a split coefficient surface would be driving with one tire in a puddle and the other on dry pavement.

tion, normalized to the maximum tractive effort when both wheels are on an equal coefficient surface. This is plotted against the ratio of the two surface coefficients for various values of the ramp coefficient, C. Maximum tractive effort is increased by increasing the ramp coefficient of the differential to provide more "lock." An similar trend would be observed if the vertical load on the two driven tires was varied through lateral load transfer, as in a turn – the differential with a higher ramp coefficient would allow greater in-line acceleration. As will be seen later, however, the ramp coefficient also has an effect on how the car handles, so a higher value might not necessarily be better.

2.3.3 Asymmetric Ramps

In most cases, it is desirable to have a different ramp angle for driving and coasting. Typically, the desired ramp angle is large for driving so that the differential is locked to maximize tractive effort. For most race cars, however, it is desirable to have an open differential when coasting (or braking) so that the differential does not impair turning. To achieve this, different ramp angles are used on the driving and braking side (see figure 2.7). When a driving torque is applied to the differential housing, the the pinion is forced against one side of the ramp, when a braking torque (from engine braking) is applied to the housing, the pinion is force against the other side of the ramp. All versions of the U of T differential have had a 45^0 ramp angle for driving and 0^0 for braking. When calculating the clutch torque with Eq 2.4,

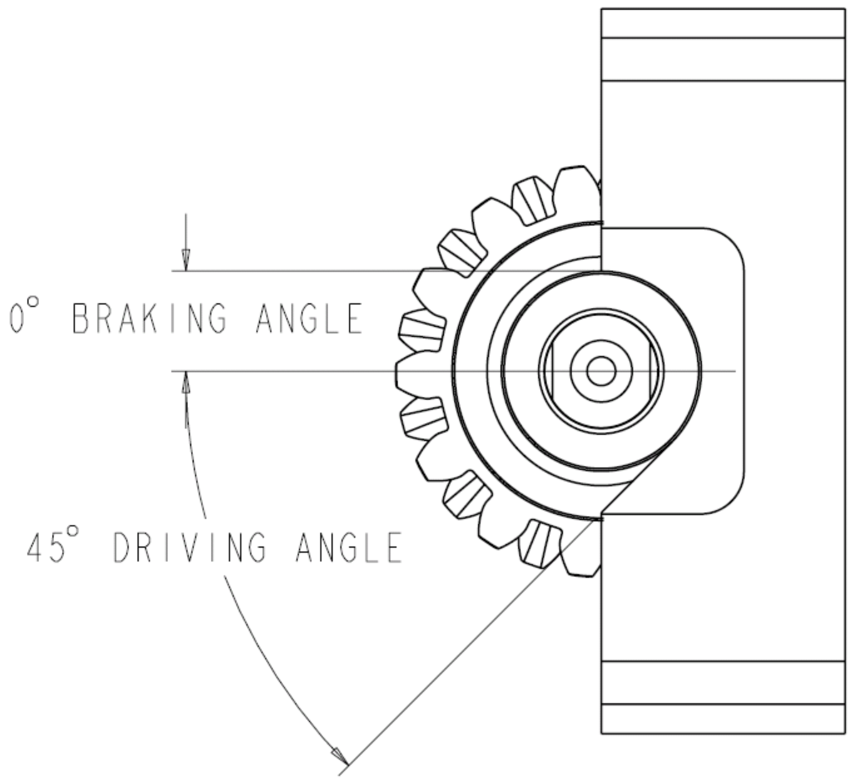

Figure 2.7: Asymmetric ramp angle

the appropriate ramp angle should be used depending on whether a driving or braking torque is applied to the differential.

2.3.4 Clutch Hysteresis and Pinion Climbing

An interesting phenomenon becomes evident upon analysis of the ramp system in a Salisbury differential. As the torque applied to the housing is increased, the the pin moves up the ramp. The friction against the ramp opposes this. Thus, the normal load on the clutch pack will be less than that predicted by Eq 2.4. Conversely, when the torque applied to the housing is reduced, the pin will tend to move down the ramp. Again, friction will resist this and the normal load on the clutch pack will be greater than that predicted by Eq 2.4. In fact, as the torque is increased and decreased, a hysteresis loop will be formed. The effect that this has on vehicle dynamics has not been investigated but might have a significant effect under certain circumstances.

Another effect caused by the friction against the ramp is an effect that can be termed "Pinion Climbing." In order to reduce the overall size of the differential, hubs on the back of the spyder gears were used to contact the ramps instead of using the spyder pin as is customary in Salisbury differentials. As the differential is differentiating, the spyder gear rotates relative to the housing and hence the ramp. When the unit is differentiating in one direction, the spyder gear will try to "climb" the ramp and hence increase the normal force on the clutch. When differentiating in the opposite direction, the rotation of the spyder gear will reduce the normal force on the clutch pack. Hence, when the differential is differentiating, its characteristics will be different for a left and a right turn. This asymmetry could potentially be exploited by a race team to obtain different handling characteristics for left and right turns. For example, when racing on a track with a right-hand hair pin and several left-hand large radius turns, a slight advantage may be seen if the differential were set up for a higher ramp coefficient for a left-hand turn. This effect, however, will not be studies further,

2.4 Adjustment Mechanism

Since this differential was designed to allow for adjustment of its parameters while installed in the vehicle, an external adjustment mechanism was devised. Pairs of pins are used to select the number of number of clutch plates that are active. These pins are notched on one side to allow the clutch plate to pass freely when the notch faces inwards. The view on the left of figure 2.8 shows the pin engaged in a clutch plate. In this configuration, the clutch plate is fixed relative to the housing and is hence transferring a torque from the housing to the adjacent clutch plates through friction. The view on the right of figure 2.8 shows the pin in the disengaged orientation. This allows the clutch plate to move relative to the housing and hence this clutch plate does not resist differentiation. Using two pair of these pins, two, four of six friction surfaces can be selected. This allows the TBR [2] of the MK III to take the discrete values of 2.0, 3.0 and 4.0. The two pairs of adjustment pins are of different lengths. The shorter of the two selects the engagement of one clutch plate, while the longer selects the engagement of two. The two pins are shown in figure 2.9 and a table showing what configurations result in each setting is given as table 2.2.

[2] The Torque Bias Ratio (TBR) is a measure of how much "lock" a differential has. It is defined as the ratio of the two half-shaft torques when the differential is differentiating. The TBR is always greater than unity.

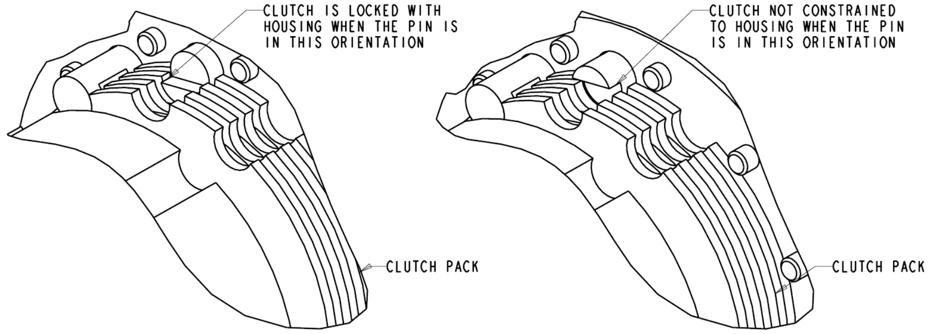

Figure 2.8: Adjustment pins in U of T differential

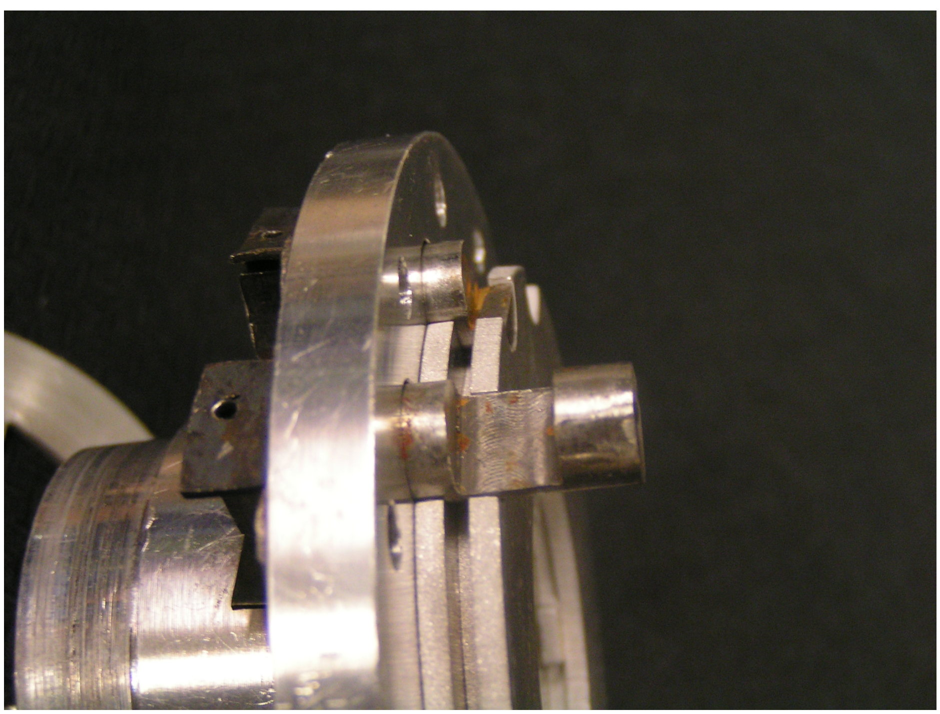

Figure 2.9: Adjustment pins, Mk II version

		Long pin	
		Notch inward	Notch outward
Short pin	Notch inward	Setting 1	Setting 3
	Notch outward	Setting 2	Setting 3

Table 2.2: Adjustment Configurations

Chapter 3

Detailed Mechanical Design

3.1 Approach

The mechanical design was preformed by first determining the required components and the way that they fit together. This was done primarily in an intuitive way. It was realized early on that the size of the gear set would dictate the size of the whole unit. Therefore, the gears were designed first. The ramp was designed next as it would affect the diameter of the differential. The clutch pack was then designed, followed by the housing and all of the remaining parts. The part of the differential are shown in figure 3.1 along with their names.

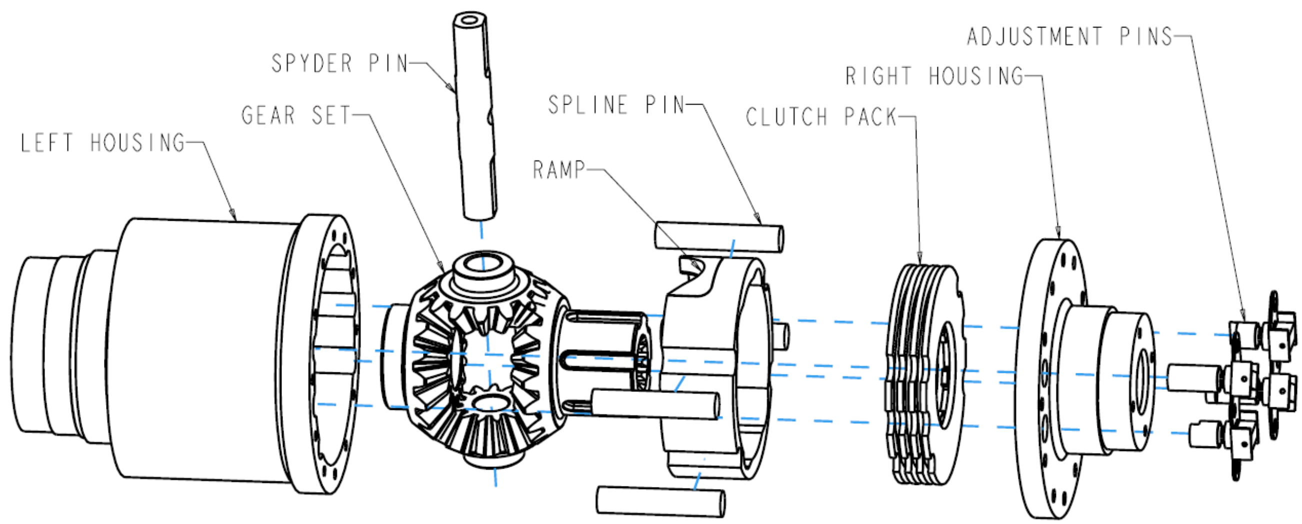

Figure 3.1: Parts of the U of T differential

3.2 Gears

3.2.1 Spur Gear Terminology

While spur gears are not used in a typical salisbury differential, their geometry is somewhat simpler than that of bevel gears, which are typically used in a salisbury differential. A brief study of spur gears is instructive since they share the same basic concepts with bevel gears.

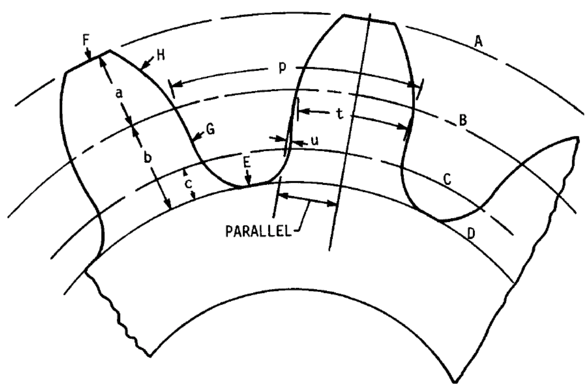

FIGURE 33.1 Terminology of gear teeth. *A*, addendum circle; *B*, pitch circle; *C*, clearance circle; *D*, dedendum circle; *E*, bottom land; *F*, top land; *G*, flank; *H*, face; a = addendum distance; b = dedendum distance; c = clearance distance; p = circular pitch; t = tooth thickness; u = undercut distance.

Figure 3.2: Figure showing main gear parameters. Figure taken from [2]

Pitch Circle: If the pair of gears were simple friction wheels (smooth wheels that don't slip relative to each other) and radius of the pitch circle is equal to the radius of the friction wheels, the friction wheels and the gears would provide the same speed ratio ($\frac{\omega_1}{\omega_2}$).

Pitch Diameter: The diameter of the pitch circle, denoted D_p.

Diametral Pitch: Diametral pitch is a measure of how big the teeth are.

Denoted DP or P_d, the diametral pitch is defined as N/D_p. Both gears in a meshing pair must have the same DP in order to mesh . There are several standard DP's: 5, 6, 8, 12, etc. The unit of in^{-1} is generally assumed when stating DP.

Pressure Angle: The angle that the tangent to the tooth profile at the pitch circle makes with a radial line passing through the same point. Denoted ϕ and specified in degrees. Both gears in mesh must have the same pressure angle. Common pressure angles are $14\frac{1}{2}$, 20 and 25.

Addendum: The portion of the tooth outside the pitch circle. Denoted a. Typical values for addendum are $1/P_d$.

Dedendum: The portion of the tooth inside the pitch circle. Denoted s. Typical values for dedendum for $14\frac{1}{2}$ degree pressure angle teeth are $1.157/P_d$.

Whole Depth: The entire depth of the tooth from tip to root $(a + s)$.

Working Depth: The part of the tooth that contacts the mating tooth. This value is always less than the whole depth, otherwise the tip of the tooth would interfere with the root of the mate. Typically, the working depth is twice the addendum.

Backlash: The clearance between two mating teeth, typically a few thousandths of an inch. This clearance allows for misalignment of the gears without binding and also allows for tooth profile error. Suggested backlash values are given in AGMA B97 [9].

Center Distance or Mounting Distance: The distance apart that two gears should be mounted to ensure proper meshing. This is equal to the sum of the pitch radii of the two mating gears.

Undercutting: If a gear has too few teeth, the profile must be modified to prevent interference of the mating gear tip with the lower part of the gear's flank. Moderate undercutting will appear as an elongated tooth; in cases of severe undercutting the root of the tooth will be narrower than the width at the pitch line, resulting in severe strength reduction.

Hunting Ratio: If the number of teeth in a pair of gears, N_1 and N_2 do not have any common divisors, a particular pair of teeth will contact each other relatively infrequently [10]. When this is the case, the gear ratio is said to be a hunting ratio. Using a hunting ratio tends to even out wear on both gear teeth, especially when slight tooth-to-tooth profile variation exists. The ratios 17:24, 13:19 and 21:12 are examples of hunting ratios, while 12:24, 14:21 and 19:38 are not.

For a full discussion of gear terminology, please refer to Cleghorn [8], Shigley [11] or Oberg [2].

3.2.2 Bevel Gears

Bevel gears are similar to spur gears with the exception that bevel gears are specified relative to a set of cones rather than circles (or cylinders) as in the case of spur gears. Instead of a pitch circle, bevel gears have a pitch cone. Also, addedendum and dedendum are usually specified as an angle, rather than a linear dimension. The basic bevel gear measurements are shown in figure 3.3. The drawing for the right side gear of the Mk III is given as appendix D and is representative of most bevel gear drawings.

Bevel gear teeth taper from the widest point at the outside edge of the gear converging to a point at the center (the apex). The pitch is given in terms of the tooth width at the outside of the gear.

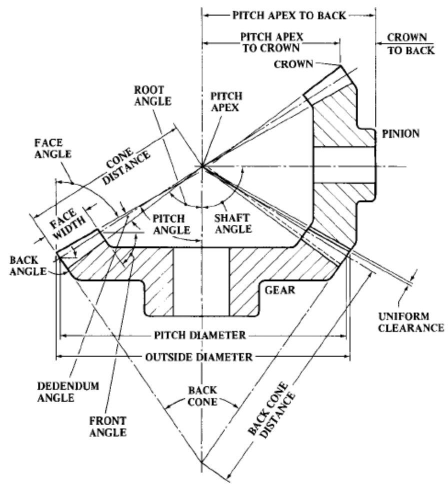

Figure 3.3:

There are several bevel gear systems. The most common is the Gleason system, which the U of T differential uses. There are a set of standard pressure angles and diametral pitches within this system. Mainly, the system determines how the gear is actually cut and how the teeth are referenced to the gear blank. In the gleason system, the gear blank is located in the cutting machine (called a generator) by referencing the face cone. The teeth are then cut with respect to the face cone. Thus, if the gleason system is used, the face cone must be accurate in terms of both angle and apex location.

The gleason system also incorporates a slight crown into the gear teeth along the width of the tooth to allow for some misalignment.

3.2.3 Gear Calculations

The gears were designed by using the calculations given in the AGMA standard for bevel gears, AGMA B97 [9]. Several design approaches were attempted before, however. First, the design rules for bevel gears presented in Shigley [11] were used. Shigley uses calculations very similar to those found in AGMA B97. The bending and contact stress numbers (defined below) are found using the factors J and I respectively – the so called geometry factors. Shigley presents the geometry factors in the form of a series of graphs, while AGMA B97 provides formulas for calculating these factors. These graphs presented in Shigley do not give the geometry factors for gears as small as those being designed, thus, this approach was abandon in favor of using AGMA B97.

A calculation sheet with the AGMA B97 calculations was created in MathCAD. This allowed for quick design iterations, as the stress number is automatically calculated each time a parameter is changed. The switch from the Shigley calculations to the AGMA calculations had the added benefit that finding the geometry factors on the graph was no longer needed for each iteration – the process became completely automated since the geometry factors can be found analytically. The MathCAD calculation sheet for the Mk III gears is given in Appendix E.

3.2.4 Allowable Stress

The strength calculations in AGMA B97 are built around the concept of a *stress number*. This number has the same units as stress, but not necessarily the same magnitude as stress. For example, ABMA B97 lists the allowable bending (tensile) stress number for Nitralloy 135M (a type of nitriding steel) as 24.0 ksi, while the tensile strength is 115 ksi [12]. This discrepancy is due to two factors. Stress is not numerically equal to stress number, and also the AGMA specifications are extremely conservative – too conservative for the design of a race car component where weight is of prime importance.

In order to arrive at a less conservative design, some commercially available differential gears were benchmarked. A test fixture was built to hold a pinion and side gear from a Yamaha Kodiak ATV front differential and apply a torque to the side gear. The torque applied to the side gear was increased until fracture of a tooth occurred. The tooth geometry of the two gears were measured and input into the AGMA B97 calculations. The bending stress number was found at the failure load. The geometry of this pair of gears and the stress number at failure are given in table 3.1.

	Pinion	Gear
Teeth	10	16
Pressure Angle	20 degrees	20 degrees
Diametral Pitch	7	7
Whole Depth	0.267 in	0.267 in
Failure Torque	2048 in-lb	3276 in-lb
Bending stress number at failure	109 ksi	164 ksi

Table 3.1: Data from benchmarked gears

To relate these results to a material allowable, a material analysis was preformed by fellow U of T Engineering student, Steven Choi. Using a mass spectrograph, the material was determined to be AISI 8620 and micro hardness testing determined that they had been carburized to a depth of approximately 0.040 inches. The material analysis is given in figure 3.2.

Element	Weight %
Carbon	0.1582
Nickel	0.12
Molybdenum	0.15
Manganese	0.7
Chromium	1.0

Table 3.2: Material analysis of benchmarked gear

3.2.5 CAD of Bevel Gears

In order to produce drawings for manufacturing, it was decided to model the bevel gears in CAD. Pro/Engineer was used. The modeling began by constructing a mathematically defined surface based on the formulas given in [13]. This surface defines the flank of one tooth. Figure 3.4 shows this surface. The flank surface was then mirrored and patterned to define the remaining tooth flanks. The material between the teeth was then cut out. The final result is shown in figure 3.5.

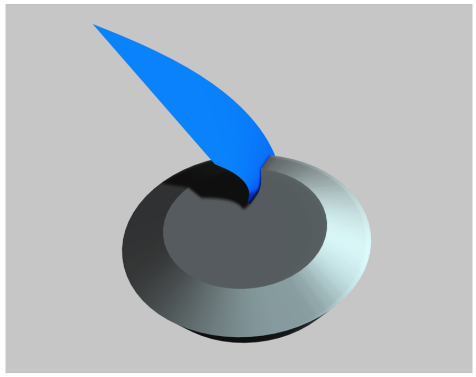

Figure 3.4: Construction surface for one gear tooth flank

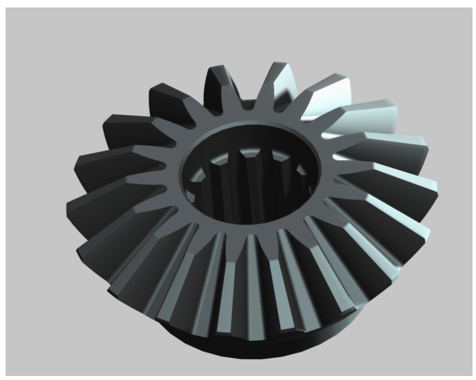

Figure 3.5: Rendering of finished bevel gear model

3.2.6 Choice of Pitch, Addendum & Dedendum

The process of searching for a minimum mass configuration for the gear set led to several general observations about the effect of various gear parameters. Unlike most gearing applications, differential gears are statically loaded [9] – when the two driven wheel speeds are equal, the gears of the differential do not move relative to each other. The AGMA specifications indicate that gears loaded statically should be designed assuming a contact ratio of 1.0, to allow for inaccuracies in the gear manufacturing that would cause only one pair of teeth to be in contact at a time.

As the number of teeth of a dynamically loaded gear is increased while keeping the pitch diameter constant, the contact ratio will increase to (approximately) offset the loss in strength due to the smaller teeth. However, when the same is done for statically loaded gears, the contact ratio stays constant at 1.0, so the reduction in tooth size means a reduction of the torque capacity of the gear. Therefore, choosing larger (and fewer) teeth for a differential gear set is preferential to choosing a large number of small teeth. Of course, if the number of teeth is decreased too far, undercutting will result, which has a far more decremental effect on gear strength.

It was found that stub teeth are preferential for differential gears because the bending stress is reduced. Stub teeth have shorter a addendum and dedendum than standard teeth, so the bending moment is reduced. Differential gears are typically designed for tip loading [9], so the reduction in whole depth is especially important to reduce the stress. For this reason, the Mk III gears were designed with stub teeth.

3.3 Ramp Design

In some salisbury differentials, the spyder pin bears directly on the ramp. This was the configuration first investigated for the Mk I. Using Hertzian contact theory, the required thickness of the ramp was very large. This thick ramp was causing the overall diameter of the differential to become excessive. Treating the pin bearing on the ramp as an infinite cylinder bearing on an infinite plate, the stress is given by Eq 3.1 taken from [14].

$$\sigma = 0.798\sqrt{\frac{p}{DC_E}} \tag{3.1}$$

Where D is the diameter of the pin, C_E is an elasticity parameter and p is the load per unit width. As can be seen from this equation, a doubling of the pin diameter and a halving of the contact width (doubling the load per unit width) would not change the stress. Thus, increasing the diameter of the pin will have an advantageous effect on the thickness of the ramp. However, doing so will force the diameter of the spyder gear to increase to fit this larger pin. To prevent this consequence, the decision was made to use a hub on the back of the spyder gear to bear on the ramp (see figure 3.6). This resulted in a significantly reduced overall diameter, but led to the "pinion climbing" phenomenon described in section 2.3.4.

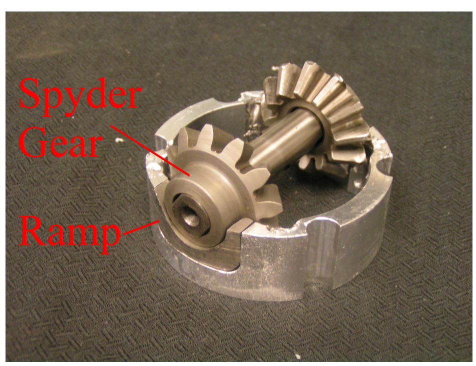

Figure 3.6: Spyder gear hub sitting in ramp

3.4 Clutch Design

The first two parameters of the clutch chosen are the inner and outer diameter of the clutch plates. These are chosen based on the gear and ramp diameter. The inner diameter is based on the the diameter of the side gear hub and the outer diameter is based on the size of the gear set and the ramps. The inner and outer diameter of the clutch pack is important because it dictates the force on the spline teeth that attach half of the plate to the side-gear and the other half to the housing. Larger diameters result in lower forces on the spline teeth.

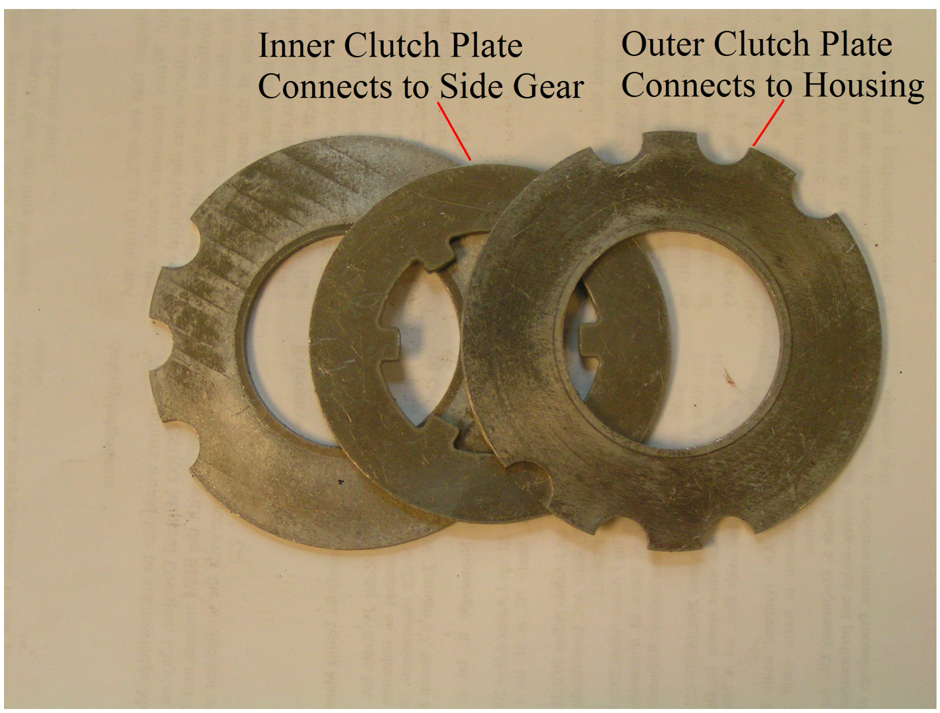

Figure 3.7: Clutch plates of Mk II

The torque on the clutch pack can be estimated through the equations presented in section 2.3.1. The torque on each clutch plate can be found from this by simply dividing by the number of clutch plates transmitting the torque. This number can then be used in the design of the spline that connects the inner clutch plates to the side gear and the outer clutch plates to the housing. Since the geometry of the clutch plates was set by packaging requirements, the two parameters that were changed during the design process were the material and the thickness.

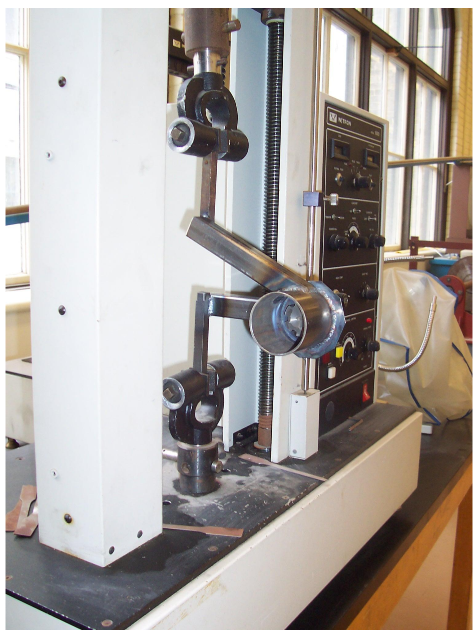

Figure 3.8: Testing of inner clutch spline

The Mk I used AISI 4130 steel clutch plates with a friction lining to provide adequate friction with low wear rates. An FEA was performed to determine the required thickness of the steel clutch plate backing. The FEA

Figure 3.9: Failed inner clutch spline. Note that all teeth are buckled sideways.

predicted that 0.035 inch thickness would be sufficient for the inner clutch plates and 0.063 inch for the outer clutch plates. In order to validate the FEA, physical testing was preformed for both the inner and outer clutch plate splines. A test spline was machined and mounted to a custom made loading fixture. This fixture mounted to a standard tensile testing machine and applied a torque to the splined connection with a moment arm. Testing of the inner clutch spline (figure 3.8) revealed an unexpected failure mode: buckling. The teeth of the spline buckled in torsion at a much lower load than required. The failed teeth are shown in figure 3.9. Further testing indicated that the clutch plate backing needed to be 0.063 inch thick instead of the originally expected 0.035 inch.

FEA of the outer clutch plates was performed with a half-model with a cyclic-symmetry constraint applied. A spline pin was modeled as well as the clutch plate backing. The friction surface of the clutch plate was constrained and the spline pin loaded. A contact region was defined between the two parts, and a implicit non-linear analysis was run with MSC.Nastran. The stress results are shown in figure 3.10. Testing of the outer clutch plates matched the FEA to within expected tolerance.

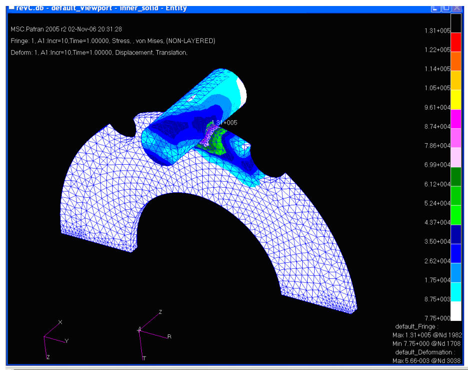

Figure 3.10: Stress results of the outer clutch spline FEA

During the design of the Mk II, David Boom, a fellow engineering student at U of T suggested using bare aluminum clutch plates to save weight. He investigated this by running the two test described above with aluminum clutch plates to obtain the required thickness. Since aluminum tends to exhibit high wear rates when run against another aluminum part [15], he also ran a wear test. This testing indicated that the clutch pack would wear less than 0.010 inches over one season – an acceptable wear rate. Changing material from steel to aluminum and removing the friction lining reduced the weight of the differential by 0.60 lb.

3.5 Housing Design

The differential housing preforms several function in the differential. First, it transfers torque from the sprocket to the ramp will allowing the ramp to slide along the axis of the differential. Secondly, it must react the separating forces from the gears[1] Third, it must transfer torque to the outer clutch plates. Fourth, it must provide a seal to keep the lubricating oil in. Finally, it must allow installation of all the components of the differential.

To accomplish the last requirement – that the housing allow for installation of all components of the differential – a two piece design was chosen (see figure 3.11).

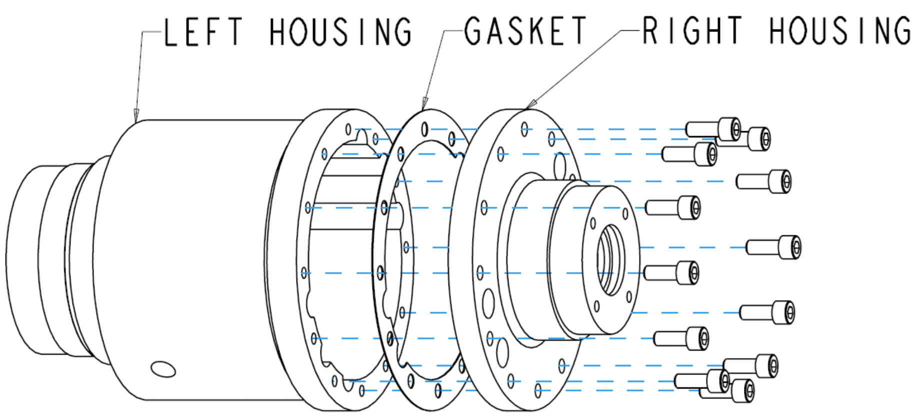

Figure 3.11: Two piece differential housing

The mechanical design of the housing was performed in several stages.

[1]Any gear in a mesh with a pressure angle greater than zero will try to separate from its mate. For bevel gears, the separating force is given by $F_s = \frac{T}{C_m} \tan\phi$ where T is the torque applied to the gear of interest, ϕ is the pressure angle and C_m is the mean pitch cone radius.

First, the basic geometry was identified and modeled in CAD. Several parameters that could be changed without affecting functionality were identified. These included wall thickness of the housing, location of the screws that fasten the left and right halves, joining flange thickness and several others. The main parameters that were varied are shown in figure 3.12 These parameters were optimized to give minimum weight with adequate strength through finite element analysis.

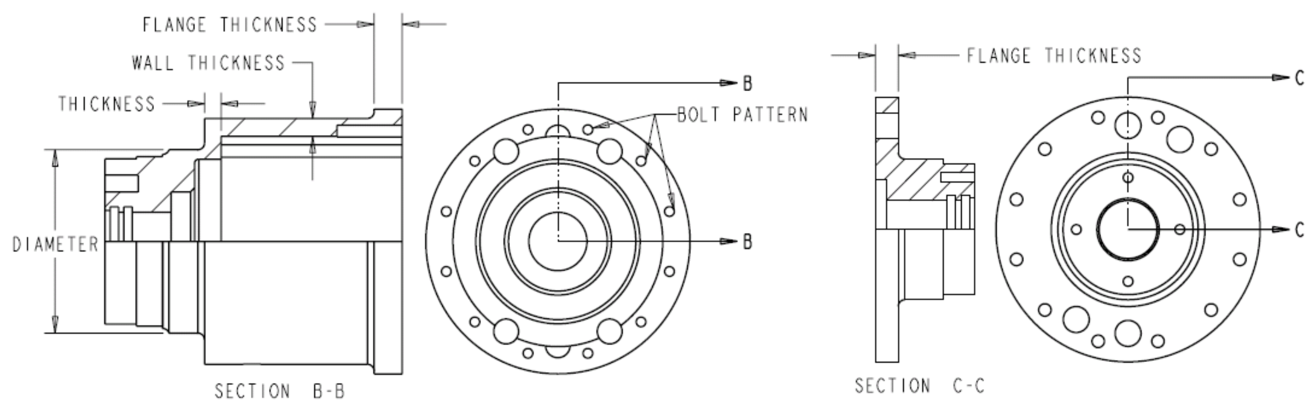

Figure 3.12: Differential housing parameters

3.5.1 Housing FEA

The housing was analyzed through a series of FEAs. The wall thickness was chosen by running a set of localized FEAs. A section of the differential hosing was modeled along with the spline pin that affixes the ramp to the housing. A tangential load was applied to the spline pin and one end of the differential housing constrained. Both the pin and the slot that if fits into were defined as deformable contact regions for an implicit non-linear analysis in MSC.Nastran (solution sequence 600 was used). The von Mises stress within the differential housing was observed and the analysis repeated for several values of wall thickness. Representative results are shown in figure 3.13. The minimum wall thickness that met the maximum allowable von Mises stress was selected.

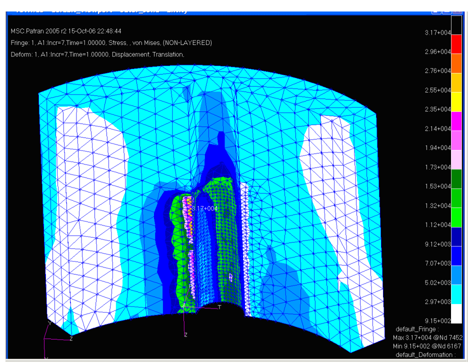

Figure 3.13: Wall thickness FEA results (stress in psi)

To optimize the other design parameters, a finite element analysis was preformed on the entire differential housing. All of the internal and external loads were applied to the housing. A contact region was defined between the two halves of the differential and the preload and elasticity of the twelve bolts joining the two halves modeled. The design parameters were adjusted to minimize the mass and keep the von Mises stress within allowable limits. Figures 3.14 and 3.15 show the von Mises stress results of this FEA for the Mk II.

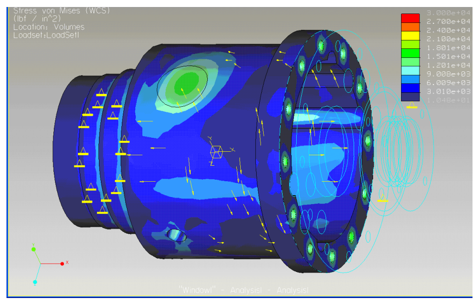

Figure 3.14: Stress results of housing FEA, left side (psi)

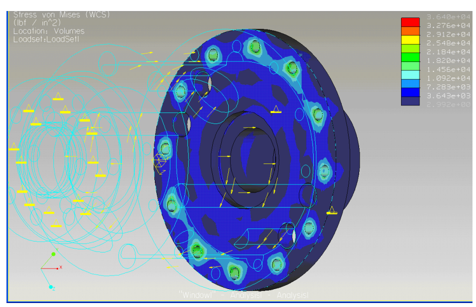

Figure 3.15: Stress results of housing FEA, right side (psi)

3.5.2 Seal Design

Ensuring that the differential will seal the lubricating oil inside is a critical aspect of the design. A leak can have two disastrous consequences: if the oil leaks out of the differential, the gears will not be properly lubricated and are more likely to suffer a contact failure such as scuffing or pitting [2]; also, a leak seen by a track martial during competition can result in disqualification of the car. There are four places in the housing that can potentially leak: the stub shafts, the adjustment pins, the joint between the right and left housing and the drain plug.

Both the stub shafts and the adjustment pins are sealed with o-rings. The glands are designed according to the design rules presented in [11]. These seals have not presented a significant problem.

The drain plug allows the differential to be filled and drained of oil. The plug itself has an NPT tapered thread and is thus self-sealing against the tapered female thread in the differential housing. It has not posed significant problems,

The joint between the left and right side of the differential housing has been a source of issues. The Mk I was sealed here with RTV silicone gasket material. An investigation into this leak led to the conclusion that the joint was flexible enough to allow certain parts to separate under the separating load from the gears. This separation was allowing oil to pass through the crack formed. Consequently, the Mk II and Mk III housings were designed to prevent this. The mating flange was made thicker and the bolt pattern op-

[2]Scuffing is a failure caused by two gears micro-welding together while rotating. These micro-welds tear and leave a damaged surface. Pitting is caused by excessive sub-surface shear stress. This causes a number of cracks join below the surface to free the material above, leaving a small pit.

timized to assure that a minimum contact pressure was maintained between the two parts over the entire surface. This was analyzed by running a finite element analysis that included all of the internal loads in the differential, the preload and stiffness of the bolts and the contact between the two halves of the differential. Figure 3.16 shows the result of this FEA for the Mk II geometry. The silicone gasket was also replaced by a rubber-infused paper gasket.

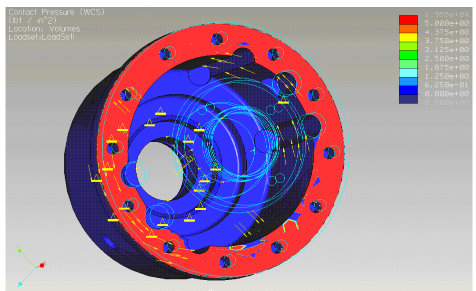

Figure 3.16: Contact pressure between two halves of differential housing. Red indicates minimum of 5 psi contact pressure.

3.6 Differential Manufacture

All three versions of the differential were manufactured in much the same way. The housings were machined by hand by members of the U of T FSAE team as were the adjustment pins, the ramps and the spyder pin. The clutch plates were cut from sheet metal using a water jet process by Profile Water jet. The gears were cut using a Gleason bevel gear generator by True Gear and Spline. The Mk I gears were designed to be nitrided, and were hence

Mk I	5.91 lb
Mk II	4.67 lb
Mk III	5.25 lb

Table 3.3: Weight of each iteration of the U of T differential

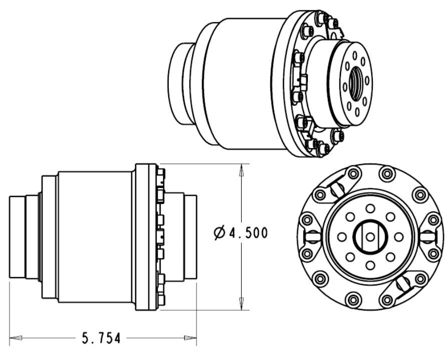

Figure 3.17: Outer dimension of the Mk I differential

hard machined and then nitrided. The Mk II and Mk III gears were designed to be carburized and were machined in the soft state prior to carburizing to a depth of 0.020 inch.

3.7 Mechanical Performance

Of the three iterations designed, two have been built and tested. Table 3.3 shows a comparison of the weights of the three units and figures 3.17 - 3.19 show the exterior dimensions of the three. The Mk I proved to be a relatively robust unit but had two failings. First it was quite heavy and second, it had a constant, slow oil leak from between the two halves of the housing.

The Mk II was redesigned with a more rigid mating flange between the

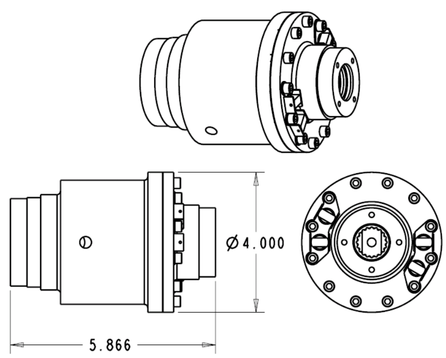

Figure 3.18: Outer dimension of the Mk II differential

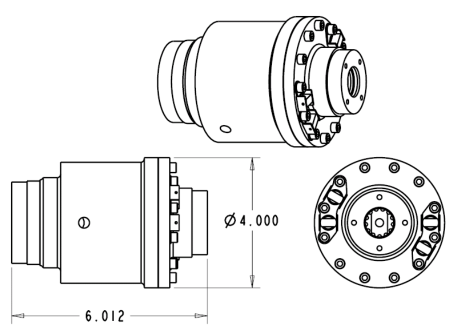

Figure 3.19: Outer dimension of the Mk III differential

left and right sides. This solved the oil leak problem. Many of the other components were redesigned as well to reduce the overall weight, which dropped by 21% over the Mk I. The Mk II suffered one issue, however. The gears experienced a fatigue failure. The spyder gear teeth fractured several times throughout the season. Figure 3.20 shows a pair of failed spyder gears. Upon investigation of this issue, it was discovered that the gear manufacturer had not cut the teeth according to the drawing. The drawings specified that the gears were to have 25^0 pressure angle teeth, but the gears were manufactured with a 20^0 pressure angle. This manufacturing error meant that the teeth were thinner at the base and hence had higher bending stress. Table 3.7 shows the stress number for the Mk II gears as they were designed and as they were built. The out-of-spec pressure angle had a considerable effect on the bending stress number.

The Mk III addresses the gear fatigue issue seen in the Mk II. The gears were redesigned as 20^0 pressure angle gears since the manufacturer chosen does not have tooling to cut 25^0 pressure angle teeth. To reduce the bending stress, the number of teeth on the side gear was increased by two and the number of teeth on the spyder gear was increased by one. As can be seen in table 3.7, the stress numbers have been reduced significantly over those seen in the Mk II, as it was manufactured.

Figure 3.20: Failed Mk II spyder gears

	Bending Stress Number		Contact stress number
	Gear	Pinion	Contact
Mk I	64 ksi	49 ksi	372 ksi
Mk II (design)	107 ksi	94.5 ksi	268 ksi
Mk II (mfg'd)	133 ksi	115 ksi	247 ksi
Mk III	139 ksi	104 ksi	246 ksi

Table 3.4: Comparison of gear stress number

Chapter 4

Vehicle Dynamics

An important metric in vehicle dynamics is the yaw moment, N. This is the moment that turns the car either in or out of a turn. A differential, by applying different torques to the left and right wheel, can produce a yaw moment. As will be seen, this can have a large effect on the handling of a car. The differential can either produce an oversteer moment[1] or an understeer moment[2].

Two approaches are used here to study the stability and control characteristics of a vehicle. First, a linear analysis is performed, followed by a non-linear vehicle dynamics analysis. Non-linear analysis tends to be more complete, but it is often more difficult to identify the effect that each parameter of the vehicle has on the handling.

[1]An oversteer moment tends to turn the car into the turn. For a right-hand turn, which is assumed in this chapter, oversteer moments are positive.

[2]Understeer moments turn the car out of a turn. For right-hand turns, an understeer moment is negative

4.1 Linear Analysis

There are two assumptions made in non-linear vehicle dynamics analysis. First, a linear tire model is assumed. This reasonably close to reality at low force levels. Referring to figure 1.2, the tire lateral force curves are reasonably close to linear at low force levels. The same is true for longitudinal force. The second assumption made is that the various effects that contribute to handling can be simply superimposed and thus do not interact. Again, this assumption is usually reasonably good for low force levels. In addition to the two assumptions stated above, there are many effects that cannot be described by a linear model. These include camber change with roll, compliance effects and the like, but once again, these effects are usually small at low force levels.

A salisbury differential is inherently non-linear, operating in two distinct ranges. In the first operating range, the torque required to overcome the friction in the clutch pack, T_c^{max} is greater than the difference in left/right drive shaft torque. In this case, the differential is effectively locked. The terms locked and spool will be used interchangeably to refer to this operating range. The second case is when there is a sufficient difference in torque between the left and right drive shafts to cause the clutch to slip. In this case, the difference between drive shaft torques will be exactly T_c^{max}. This operating range occurs when the differential is differentiating, and will be referred to as such. In order to derive a linear model of this inherently non-

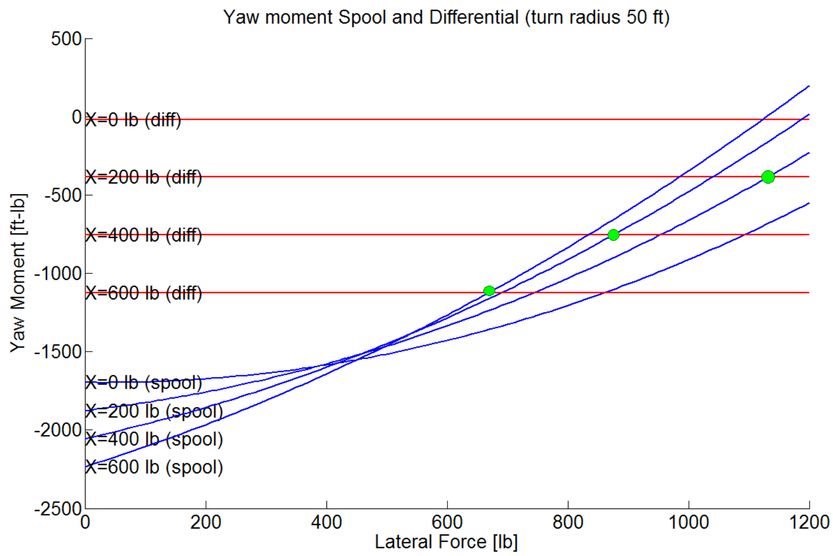

Figure 4.1: Yaw moment produced by a differential and a spool. Greed dots indicate transition points between locked and differentiating operation.

linear device, the two operating ranges will be studied separately.

When the differential is locked, the yaw moment produced is given by Eq 4.1 and when the differential is differentiating, the yaw moment becomes Eq 4.2. Both of these expressions are derived in Appendix C. The yaw moment for both cases is plotted against lateral force, Y, for both cases in figure 4.1.

$$N^{spool} = \left[\frac{2V\rho hY}{r} - t^2\left(F_{z0} + hX/\left(2w\right)\right)\right]\frac{r\left(X + 2C_x\left(F_{z0} + hX/\left(2w\right)\right)\right)}{2V\left(F_{z0} + hX/\left(2w\right)\right) - \rho hY} - 2C_x\rho hY \tag{4.1}$$

$$N^{diff} = \frac{-tT_c}{R_t} = \frac{-t\left(CXR_t + B\right)}{R_t} \tag{4.2}$$

It is interesting to note that, at least based on this linear model, a salisbury differential only provides yaw-damping when operating as a spool; when it is differentiating, the yaw-moment is independent of yaw-rate.

Since tire radius is assumed constant in this model, the yaw moment produced by the differential is proportional to the difference in left and right drive shaft torque. Therefore, the limiting difference in left/right torque, T_c^{max} can be translated into a limiting yaw moment. This limiting yaw moment defines the point where the differential will transition from acting as a spool to differentiating. These transition points occur when $N^{spool} = N^{diff}$ and are shown as in figure 4.1. At a given in-line force, X, the differential will impart a yaw moment that remains constant as lateral force is increased until a critical lateral acceleration, at which point, the differential will transition from differentiating and become locked. The yaw moment will increase (become less negative) and will actually impart an turn-in (oversteer) moment at a sufficiently high lateral force.

The increasing yaw moment with increasing lateral force for the case of a spool is due to lateral load transfer. As the outside wheel becomes more highly loaded and the inside less loaded, the outside tire has more tractive capacity. The yaw moment produced by the increased in-line force on the outside wheel becomes sufficient at a certain point to overcome the drag from the inside wheel caused by its lower slip ratio.

The critical lateral force at which the differential will transition from differentiating to being locked is shown in figure 4.2. As the in-line force is

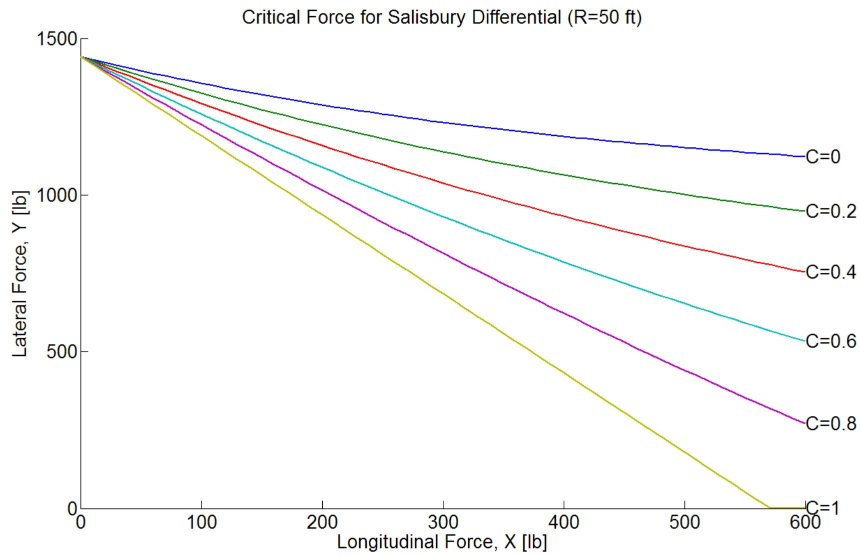

Figure 4.2: Critical lateral force to lock a salisbury differential. Various values of C shown. Preload kept constant at $4.11 ft \cdot lb$.

increased, the differential will become locked at a decreasing lateral force. This effect is increased as the C value of the differential is increased.

4.2 Non-linear Analysis

In order to remove some of the assumptions made in the linear model, a non-linear model was created. This model uses a non-linear tire model based on the Pacejka '96 model. Lateral and longitudinal force data was obtained through laboratory testing at Calspan's TIRF facility as part of the FSAE Tire Testing Consortium (TTC). The raw data was fit for the Pacejka '96 model by Stackpole Engineering Services. For more details about the model, the reader is referred to [16] and [5].

The model outputs applied torque, T_{app} and the yaw moment created by the differential, N^{diff} by sweeping through several lateral acceleration steps and through a parameter termed axle-slip, which is is defined much like slip ratio, but uses the differential housing speed, Ω, rather than wheel speed and uses the unloaded tire radius, R_t instead of the loaded tire radius. It is defined as:

$$AS = \frac{\Omega R_t}{V} - 1 \tag{4.3}$$

Several simplifying assumptions are made in the model which will affect its fidelity. First, the suspension kinematics are ignored. Constant camber and toe angle are assumed, as well as a constant motion ratio between wheel and spring. Also, geometric weight transfer is neglected[3]. These two simplifications affect the vertical loads on the tires and the angles that they are presented to the road. They will affect the handling of the car in the simulation but are not expected to affect the trends caused by the differential.

4.2.1 Observations from the Non-Linear Model

Figure 4.3 shows the results of the non-linear vehicle dynamics model. The curves for each setting exhibit slope discontinuity. This occurs at the point

[3]Geometric weight transfer arises from the suspension kinematics. The roll moment caused by the lateral acceleration, applied at the vehicle CG is reacted both through vertical loads through the suspension springs, but also directly through the suspension linkage. The component that is reacted through the suspension linkage is termed geometric weight transfer and the component reacted through the springs is elastic weight transfer.

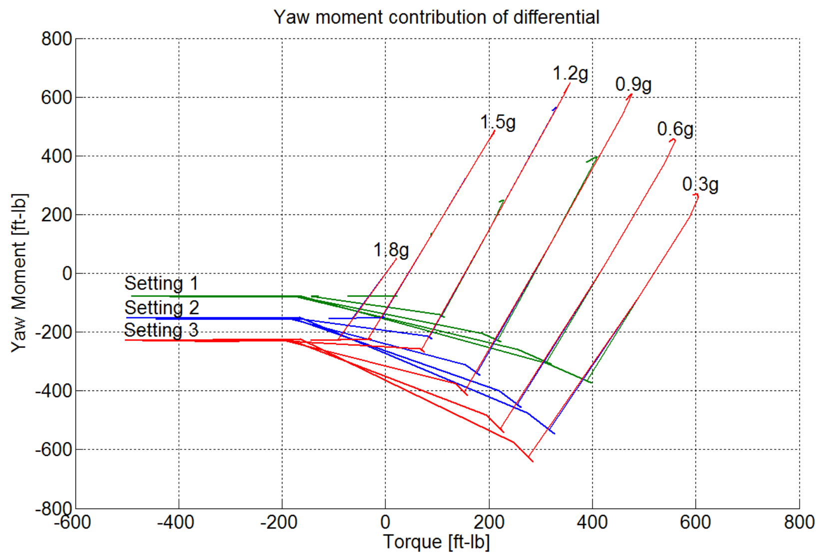

Figure 4.3: Non-linear model output: Yaw moment versus torque for various lateral accelerations and differential settings

where the differential transitions from differentiating to acting as a spool. Similar trends are observed with the non-linear model and the linear model. In the differentiating operating range, as torque (or in-line force) is increased, the yaw moment becomes more negative. As the differential transitions to spool operation, the yaw moment begins to increase and becomes positive at some point.

Also visible in figure 4.3 is the relative magnitudes of the yaw moments produced by the three differential settings. Setting 3 (the high-lock setting) produces the largest understeer moment, but also produces the highest over-steer moment. This large range would allow the driver to "steer with the throttle" – to alter the heading of the car by changing the throttle application. Also, the high-lock setting allows greater amounts of torque to be applied to the wheels: the same conclusion made in section 2.3.2.

The two models, however, do not match in numeric values. For example, comparing the transition point to locked operation for setting 2 (which corresponds to $C = 0.48$) at a lateral acceleration of 0.9 g: the non-linear model predicts that this transition will occur at $182ft \cdots lb$. Given the tire radius and vehicle mass, this corresponds to $X = 218lb$ for $Y = 567lb$. The linear model predicts that this will occur at approximately $X = 1200lb$. Also, the magnitudes of yaw-moment produced do not match. For example, the non-linear model predicts that the yaw-moment can range from $-650ft \cdot lb$ to $650ft \cdot lb$, while the linear model predicts a range of $-1200ft \cdots lb$ to $200ft \cdot lb$ for the same torque and lateral acceleration range.

Since neither model has been fully validated through testing, neither model can be said for sure to be more accurate than the other. The basic trends in each model, however, agree.

4.3 Track Data Analysis

In order to qualitatively validate the above models, on-track testing was performed. A track was set up and the 2006 U of T FSAE car, fitted with the Mk I differential drove the track. Many laps (10-20) were run for each of the three settings of the differential. The fastest lap for each setting is used in the analysis. A map of the track, broken into ten sectors, is given in figure

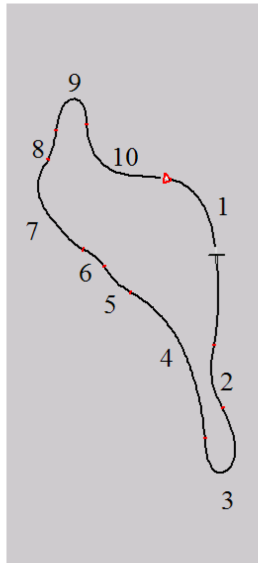

Figure 4.4: Map of track used in testing with sectors identified

4.4.

At the time of testing, some of the sensors required for a full quantitative model validation were not available. Such a validation would, at a minimum, require lateral and longitudinal accelerometers, a gyro to measure yaw-rate, a steering position sensor and a body slip angle sensor. Since a body slip angle sensor and a gyro were not available, a qualitative validation was performed instead. This, of course, can only validate the trends seen, and not numbers.

To asses the effects of the differential settings, in-line acceleration traces for each lap are compared, along with driver comments for the three settings. Figure 4.5 shows the in-line acceleration versus track position for the hairpin (sector 3). The maroon trace is the high-lock setting, the amber trace is the medium setting and the green trace is the low-lock setting. Taking note of

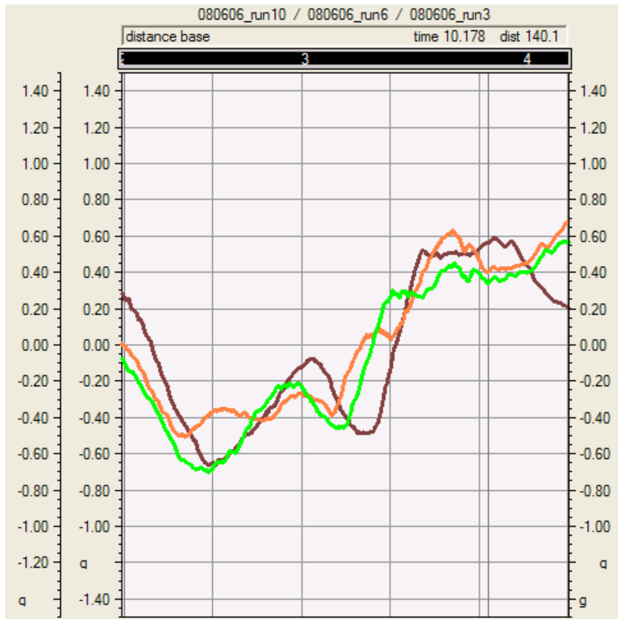

Figure 4.5: In-line acceleration, sector 3

where these three traces cross zero longitudinal acceleration, from braking (negative) to acceleration (positive), it becomes clear that the high-lock setting prevents the driver from beginning to accelerate as early as the other settings. This can be explained by the high turn-in yaw moment that the differential creates at the high-lock setting at higher lateral accelerations. The driver must reduce the lateral acceleration before beginning to accelerate in order to prevent the car from spinning out. For this tight corner, the driver is able to begin to accelerate much earlier with the low-lock setting.

Figure 4.6 shows the in-line acceleration traces for sector 10: a large radius turn. Here, the trend is opposite that seen in sector 3. Here, the driver appears to be able to accelerate earlier because, as predicted in section

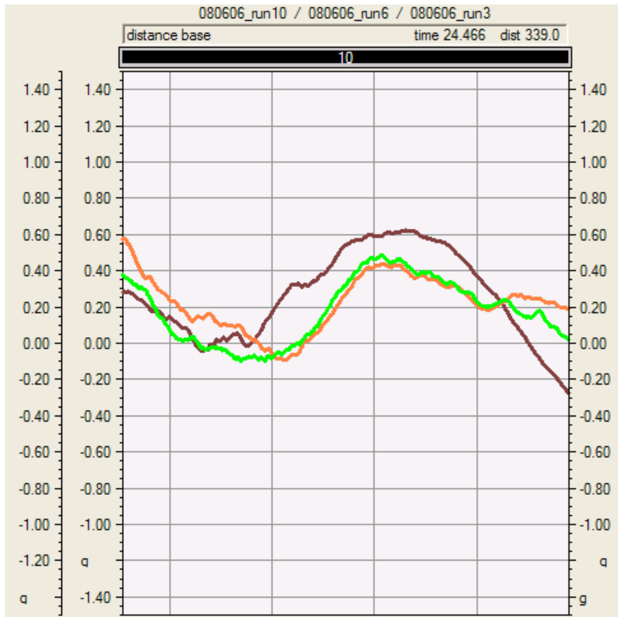

Figure 4.6: In-line acceleration, sector 10

2.3.2, the high-lock differential is able to accelerate the car while there is still significant lateral load transfer. Since this is a relatively large radius corner, the yaw moment caused by the differential is relatively low.

The general consensus among the various drivers who have driven multiple differential settings is that the car is loose (oversteer) when on throttle when the differential is at the higher lock settings. The more experience drivers tend to prefer the differential to be set at higher settings than less experienced drivers, presumably because the higher-lock settings are harder to drive, but allow the driver to "steer with the throttle" – to adjust the heading of the car by applying more or less throttle.

Chapter 5

Conclusion

It has been found, both through simulation and track testing, that the differential can have a large effect on the performance of a race car. It was found that high-lock differentials allow for greater in-line acceleration but when power is applied during a turn, an oversteer yaw moment can be generated. Track testing suggests that these two effects have opposite performance effects for large radius and tight turns. For large radius turns, the gains in longitudinal acceleration for a high-lock differential are of greater benefit than the large yaw moment is a detriment. However, for tight turns, the large yaw moment created by the differential forces the driver to accelerate out of the turn much later in order to prevent spinning-out.

Despite a few mechanical failures of the first two iterations of the differential designed for the U of T Formula SAE car, the design is converging to a reliable one. Finite element analysis, hand calculations and physical testing were used for the design, which is being constantly refined based on its mechanical performance.

The differential designed is a salisbury differential with an adjustable clutch pack. This adjustability makes for an excellent research tool, but the benefits go far beyond this. The easy adjustability means that it is feasible to make adjustments to the differential for different tracks or for different events of the Formula SAE competition. In fact, the U of T FSAE team has been doing this with definite gains.

Bibliography

[1] P. Haney, *The racing & high-performance tire.* SAE, 2003.

[2] E. Oberg, *Machinery's Handbook.* Industrial Press, 27th edition ed., 2004.

[3] S. E. Chocholek, "The development of a differential for the improvement of traction control," *IMechE*, 1988.

[4] C. Smith, *Drive to Win: The Essential Guide to Race Driving.* Carrol Smith Consulting, 1996.

[5] H. Pacejka, *Tire and Vehicle Dynamics.* SAE, second ed., 2006.

[6] W. F. Milliken, *Equations of Motion: Adventure, Risk and Innovation: The engineering Autobiography of William F. Milliken.* Bentley, 2006.

[7] W. Milliken and D. Milliken, *Race car vehicle dynamics.* Society of Automotive Engineers, 1995.

[8] W. L. Cleghorn, *Mechanics of Machines.* Oxford University Press, 2005.

[9] *Rating the pitting resistance and bending strength of generated straight bevel, zerol bevel and spiral bevel gear teeth (ANSI/AGMA 2003-B97).* AGMA, 2003.

[10] A. Stokes, *Manual Gearbox Design.* Butterworth-Heinemann, 1992.

[11] J. E. Shigley and C. R. Mischke, *Standard handbook of machine design.* McGraw Hill, second ed., 1996.

[12] "Latrobe nitralloy n vacarc premium nitriding steel." Internet: http://www.matweb.com/search/DataSheet.aspx?MatID=19357, 2008.

[13] E. Litvin, A. Wang, and R. Handschuh, "Computerized generation and simulation of meshing and contact of spiral bevel gears with improved geometry," *Computer Methods in Applied Mechanical Engineering*, 1998.

[14] W. Young and R. Budynas, *Roark's Formulas for Stress and Strain.* McGraw-Hill, 7th edition ed., 2002.

[15] R. Norton, *Machine Design, an intergrated approach.* Pearson Education, 2005.

[16] H. Pacjeka, "The tyre as a vehicle component," *FISITA Transactions CD-ROM*, 1996.

[17] R. Limpert, *Brake Design and Safety.* Society of Automotive Engineers, second edition ed., 1999.

Appendix A

Derivation of Salisbury Clutch Characteristics

This appendix shows the variation of T_c with applied torque, T, for a salisbury differential. Refer to figure 2.2 for some of the force definitions.

$$F_t = T/r_r \tag{A.1}$$

Where r_r is the mean distance from the center of the differential to the ramp.

$$F_a = \frac{F_t}{\tan\alpha} = \frac{T}{r_r \tan\alpha} \tag{A.2}$$

Where α is the ramp angle.

$$T_c^{max} = N_c \mu_c r_c \left(F_a + F_{pre}\right) \tag{A.3}$$

Where N_c is the number of friction surfaces, μ_c is the coefficient of friction of the clutch plates, r_c is the mean radius of the clutch plates and F_{pre} is the clutch preload force.

$$T_c^{max} = N_c \mu_c r_c \left(\frac{T}{r_r \tan \alpha} + F_{pre}\right) \tag{A.4}$$

Note that the force applied to the ramp is related to the torque applied to the gears, so this will be less than the torque applied to the differential, T_app, by the value of the clutch torque, T_c. With this in mind, the clutch torque, as a function of applied torque is:

$$T_c^{max} = \frac{C_A T_{app} + N_c r_c \mu_c F_{pre}}{1 + C_A} \tag{A.5}$$

Where

$$C_A = \frac{N_c r_c \mu_c}{r_r \tan \alpha} \tag{A.6}$$

The mean friction radius, r_c is given by [17] as:

$$r_c = \frac{1}{3} \frac{d_o^3 - d_i^3}{d_o^2 - d_i^2} \tag{A.7}$$

Where d_o and d_i are the outer diameter and inner diameter of the friction surfaces on the clutch plates respectively.

Appendix B

Equations for the Torque Path

This derivation shows the torque seen by each component of the differential. The left and right drive shaft torques, T_l and T_r are a function of the applied torque, T_{app} and the clutch torque, T_c.

$$T_{app} = T_g + T_c = T_l + T_r \tag{B.1}$$

$$T_{lg} = T_{rg} = \frac{T_g}{2} \tag{B.2}$$

$$T_r = T_{rg} + T_c = \frac{T_g}{2} + T_c \tag{B.3}$$

$$T_l = T_{app} - \frac{T_g}{2} - T_c \tag{B.4}$$

$$T_l = T_{app} - \frac{T_{app} - T_c}{2} - T_c \tag{B.5}$$

$$T_l = \frac{T_{app}}{2} - \frac{T_c}{2} \tag{B.6}$$

$$T_r = T_app - T_l = T_{app} - \frac{T_{app}}{2} + \frac{T_c}{2} \tag{B.7}$$

$$|\Delta T| = |T_r - T_l| = T_c \tag{B.8}$$

The torque bias ratio is the ratio of the higher:lower drive shaft torque. It is:

$$TBR = \frac{T_r}{T_l} = \frac{T_{app}/2 + T_c/2}{T_{app}/2 - T_c/2} \tag{B.9}$$

$$TBR = \frac{T_{app} + T_c}{T_{app} - T_c} \tag{B.10}$$

Appendix C

Derivation of Linear Vehicle Model

The yaw moment due to longitudinal force from the driven wheels is:

$$N^{spool} = t(F_{xl} - F_{xr}) \tag{C.1}$$

Assuming a linear tire model:

$$F_x = C_x F_z \kappa \tag{C.2}$$

Combining these equations:

$$N^{spool} = C_x t \left[F_{zl} \left(\frac{\Omega R_t}{r\,(R + t/2)} - 1 \right) - F_{zr} \left(\frac{r \Omega R_t}{R - t/2} - 1 \right) \right] \tag{C.3}$$

The vertical load on the driven tires are not independent. We'll define the constant F_{z0} as the static load on each driven tire (assumed equal) and ΔF_z as the weight transfer.

$$F_{zl} = F_{z0} + \Delta F_z^{lat} + \Delta F_z^{long} \tag{C.4}$$

$$F_{zr} = F_{z0} - \Delta F_z^{lat} + \Delta F_z^{long} \tag{C.5}$$

Of course, ΔF_z^{lat} and ΔF_z^{long} are not independent, but are dependent on the lateral and longitudinal force on the vehicle, Y and X; the height of the center of gravity, h; the fraction of anti-roll torque on the driven axle, ρ; the track, t; and the wheelbase, w.

$$\Delta F_z^{lat} = \frac{\rho h Y}{t} \tag{C.6}$$

$$\Delta F_z^{long} = \frac{hX}{2w} \tag{C.7}$$

Combining these and simplifying:

$$N^{spool} = \frac{C_x \Omega R_t}{r\left(R^2 - t^2/4\right)}\left[2R\rho hY - t^2\left(F_{z0} + \frac{hX}{2w}\right)\right] - 2C_x\rho hY \tag{C.8}$$

The longitudinal force is:

$$X = F_{xl} + F_{xr} \tag{C.9}$$

$$X^{spool} = \frac{C_x \Omega R_t}{r\left(R^2 - t^2/4\right)} \left[2R\left(F_{z0} + hX/\left(2w\right)\right) - \rho hY\right] - 2C_x\left(F_{z0} + hX/\left(2w\right)\right) \tag{C.10}$$

Solving for Ω and back-substituting, the equation for yaw moment of the spool is:

$$N^{spool} = \left[2R\rho hY - t^2\left(F_{z0} + hX/\left(2w\right)\right)\right] \frac{X + 2C_x\left(F_{z0} + hX/\left(2w\right)\right)}{2R\left(F_{z0} + hX/\left(2w\right)\right) - \rho hY} - 2C_x\rho hY \tag{C.11}$$

It appears that yaw-rate, r, does not appear in the expression for yaw moment. However, if turn radius, R, is replaced by V/r, then yaw rate now appears again. After this substitution, the yaw moment becomes:

$$N^{spool} = \left[\frac{2V\rho hY}{r} - t^2\left(F_{z0} + hX/\left(2w\right)\right)\right] \frac{r\left(X + 2C_x\left(F_{z0} + hX/\left(2w\right)\right)\right)}{2V\left(F_{z0} + hX/\left(2w\right)\right) - \rho hY} - 2C_x\rho hY \tag{C.12}$$

The stability and coupling derivatives for the spool are:

$$\frac{\partial N^{spool}}{\partial r} = \frac{t^2}{2} \frac{\left(Xw + 2C_x F_{z0} w + C_x hX\right)\left(2F_{z0} w + hX\right)}{-2VF_{z0}w^2 - VhXw + \rho hYw^2} \tag{C.13}$$

$$\frac{\partial N^{spool}}{\partial Y} = \frac{X + 2C_x\left(F_{z0} + \frac{hX}{2w}\right)}{2V\left(F_{z0} + \frac{hX}{2w}\right) - \rho hY}\left\{2V\rho h + r\rho h\frac{\frac{2V\rho hY}{r} - t^2\left(F_{z0} + \frac{hX}{2w}\right)}{2V\left(F_{z0} + \frac{hX}{2w}\right) - \rho hY}\right\} - 2C_x\rho h \tag{C.14}$$

If the differential clutch pack is taken into consideration, there is a limit to the yaw moment generated. When the differential is differentiating, the difference in right and left wheel torques is defined by the differential parameters and the applied torque (which is proportional to the in-line acceleration). The torque differential is:

$$\Delta T = T_c = CT_{app} + B = (CXR_t + B) \tag{C.15}$$

Therefore, the yaw moment generated is:

$$N^{diff} = \frac{-tT_c}{R_t} = \frac{-t\left(CXR_t + B\right)}{R_t} \tag{C.16}$$

The negative sign in the above equation arises from the definition that a positive yaw moment as a torque that tends to turn the car to the right. Since, at least at low accelerations, the outside wheel spins faster than the inside, the torque transfer from the friction of the clutch plates will be from the outside to the inside, resulting in a negative yaw moment in the case of a right hand turn.

The yaw moment gradients are:

$$\frac{\partial N^{diff}}{\partial r} = 0 \tag{C.17}$$

$$\frac{\partial N^{diff}}{\partial X} = -tCR_t^2 \tag{C.18}$$

$$\frac{\partial N^{diff}}{\partial Y} = 0 \tag{C.19}$$

The difference in left/right torque is related to the yaw moment by the tire radius and track (assuming constant tire radius and track). Therefore, if the yaw moment that a salisbury differential produces cannot exceed (in magnitude) the yaw moment given by Eq C.16. The point where this happens, the clutch will be at a state of impending slip. This will be termed the critical point for the differential and is signified by $N^{spool} = N^{diff}$.

Appendix D

Sample Gear Drawing for the Mk III

REV	DATE	DESCRIPTION	LOC	APR
C	30-SEPT-2007	CHANGE TO STUB TEETH, CHANGE NUMBER OF TEETH	--	SK
B	8-AUG-2007	CHANGE ADDENDUM/DEDENDUM	--	SK
A	1-JAN-2007	INITIAL RELEASE	--	SK

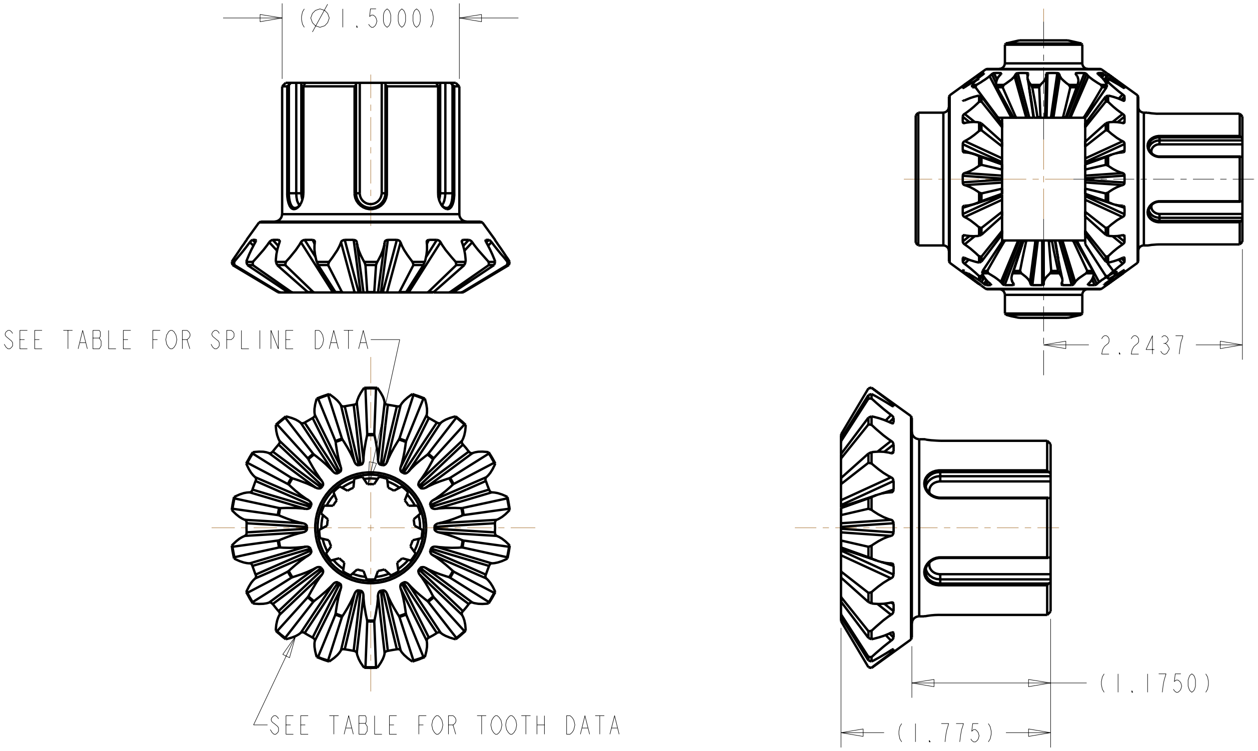

GEAR TOOTH DATA

GEAR TYPE	STRAIT BEVEL
TOOTH FORM	CONIFLEX
NUMBER OF TEETH	18
NUMBER OF TEETH IN MATE	13
DIAMETRAL PITCH	8.000
SHAFT ANGLE	(90°)
PRESSURE ANGLE	20.000°
PITCH ANGLE	(54.2°)
ADDENDUM ANGLE	5.1°
ADDENDUM	(0.125)
DEDENDUM ANGLE	5.1°
DEDENDUM	(0.125)
MINIMUM AGMA QUALITY	11
BACKLASH	0.004
TOOTH FILLET RADIUS	0.052

SPLINE DATA

NUMBER OF TEETH	13
SPLINE PITCH	16 / 32
PRESSURE ANGLE	30°
SPLINE FORM	INVOLUTE

Formula SAE Racing University of Toronto	RIGHT SIDE GEAR			SHEET 1 OF 1
S. KLOPPENBORG 416-946-3932 klopen@ecf.utoronto.ca	MACHINE TOLERANCE		DRW NO: DRIVETRAIN-DIFF-RSIDEGEAR	DATE 30-SEPT-2007
	FRAC ±1/32	.000 ±.005	MAT'L: AISI 8620 STEEL REV C	SCALE 1.000 DO NOT SCALE DRAWING
	.00 ±.010	.0000 ±.001	FINISH:	INCHES UNLESS SPECIFIED
	BREAK SHARP CORNERS 1/32 x 45° UNLESS NOTED	MINIMUM RADIUS 1/32	WEIGHT: 0.866	

Appendix E

Bevel Gear Calculations

Calculation Sheet

Title:	Differential Gear Calculations		
Calculation By:	Stefan Kloppenborg		
Vehicle Section:	Drivetrain	Sub Assembly:	2008 Differential
Component:	Gear Set	Part Number:	
Date Created:	23-MAY-2006	Date Modified:	9-Sept-2007
Calculation Rev:	A	Part Rev:	NR

All of the below calculatios are based on AGMA Standard 2003 B97 and are only valid for appplications with very low pitch line speeds, like an automotive differential. Furthermore, it is only valid for gears without profile shift.

Functional Parameters

$T_{app} := 11000\,in\cdot lbf$ Torque Applied to the differential casing

$N_p := 2$ The number of spyder gears used

Gear Parameters

$P_d := 8\cdot in^{-1}$ Diametral Pitch of both members

$Z_g := 18$ Number of teeth, side gear

$Z_p := 13$ Number of teeth, spyder gear

$\phi := 20deg$ Pressure Angle

$F_G := .475in$ Gear Facewidth, must be no smaller than F_{max}

$F_P := .475in$ Pinion Facewidth, must not be smaller than F_{max}

$F := .475in$ Facewidth: use the smaller of the above two

$backlash := .004in$ Backlash in gear mesh

$r_{TP} := .045in$ Tool Edge Radius for Pinion

$r_{TG} := .045in$ Tool Edge Radius for Gear

Material Properties

$E_g := 29\cdot 10^6 psi$ Elastic Modulus, side gear

$E_p := 29\cdot 10^6 psi$ Elastic Modulus, spyder gear

$\nu_g := .32$ Poisson's Ratio, side gear

$\nu_p := .32$ Poison's Ratio, spyder gear

$H_g := 60$ HRC harness of gear

$H_p := 60$ HRC hardness of spyder

Functional Relations

$T_g := \frac{T_{app}}{2 \cdot N_p}$ Side gear torque at each gear mesh $T_g = 2.75 \times 10^3\,in \cdot lbf$

$T_p := T_g \cdot \frac{Z_p}{Z_g}$ Pinion torque at each gear mesh $T_p = 1.986 \times 10^3\,in \cdot lbf$

Gear Relations

$D_g := \frac{Z_g}{P_d}$ Pitch Diameter, gear $D_g = 2.25\,in$

$D_p := \frac{Z_p}{P_d}$ Pitch Diameter, pinion $D_p = 1.625\,in$

$\Gamma_p := \mathrm{atan}\left(\frac{Z_p}{Z_g}\right)$ Pitch Cone Angle, spyder gear $\Gamma_p = 35.838\,deg$

$\Gamma_g := \frac{\pi}{2} - \Gamma_p$ Pitch Cone Angle, side gear $\Gamma_g = 54.162\,deg$

$C := \frac{D_g}{2 \cdot \sin(\Gamma_g)}$ Pitch Cone Radius $C = 1.388\,in$

$$F_{max} := \begin{cases} \frac{C}{3} & \text{if } \frac{C}{3} < \frac{10}{P_d} \\ \frac{10}{P_d} & \text{otherwise} \end{cases}$$

Largest Permissible Face Width $F_{max} = 0.463\,in$

Addendum and Dedendum

Addednum

$$S_1 := \frac{.540}{P_d} + \frac{.450}{P_d \cdot \left(\frac{Z_g \cdot \cos(\Gamma_p)}{Z_p \cdot \cos(\Gamma_g)}\right)}$$

$S_1 = 0.097\ in$

Dedendum

$b_1 := \frac{2.188}{P_d} - S_1$ $b_1 = 0.177\ in$

$S_2 := \frac{2}{P_d} - S_1$ $\quad S_2 = 0.153\ in$ $\quad b_2 := \frac{2.188}{P_d} - S_2$ $\quad b_2 = 0.12\ in$

$S_g := \frac{1.8}{2.118} S_1$ $\quad S_p := \frac{1.8}{2.188} S_2$ $\quad b_g := \frac{1.8}{2.118} b_1$ $\quad b_p := \frac{1.8}{2.118} b_2$

$O_g := D_g + 2 \cdot S_g \cdot \cos(\Gamma_g)$ Outside diameter, side gear $O_g = 2.346\ in$

$O_p := D_p + 2 \cdot S_p \cdot \cos(\Gamma_p)$ Outside diameter, spyder gear $O_p = 1.829\ in$

<u>Pitting Formulae</u>

$C_m := C - .5 \cdot F$ Mean Pitch Cone Distance $C_m = 1.15\ in$

$k := \frac{Z_g - Z_p}{3.2 \cdot Z_g + 4.0 \cdot Z_p}$ Location Constant $k = 0.046$

$P_m := \frac{C}{C_m} \cdot P_d$ Mean Transverse Diametral Pitch $P_m = 9.652\ in^{-1}$

$p := \frac{\pi}{P_d}$ Outer Transverse Circular Pitch $p = 0.393\ in$

$p_N := \frac{C_m}{C} \cdot p \cdot \cos(\phi)$ Mean Normal Base Pitch $p_N = 0.306\ in$

$p_n := \frac{p_N}{\cos(\phi)}$ Mean Normal Circular Pitch $p_n = 0.325\ in$

$p_2 := \frac{p_n}{\cos(\phi) \cdot \tan(\phi)^2}$ $p_2 = 2.615\ in$

$r := \frac{D_p}{2 \cdot \cos(\Gamma_p)} \cdot \frac{C_m}{C}$ Mean Transverse Pinion Pitch Radius $r = 0.831\ in$

$R := \frac{D_g}{2 \cdot \cos(\Gamma_g)} \cdot \frac{C_m}{C}$ Mean Transverse Gear Pitch Radius $R = 1.593\ in$

$r_{bN} := r \cdot \cos(\phi)$ Mean Normal Pinion Base Radius $r_{bN} = 0.781\ in$

$R_{bN} := R \cdot \cos(\phi)$ Mean Normal Gear Base Radius $R_{bN} = 1.497\ in$

$r_{oN} := r + S_p - .5 \cdot F \cdot \frac{S_p}{C}$ Mean Normal Pinion Outside Radius $r_{oN} = 0.935\ in$

$R_{oN} := R + S_g - .5 \cdot F \cdot \frac{S_g}{C}$ Mean Normal Gear Outside Radius $R_{oN} = 1.661\ in$

$$Z_{p1} := \sqrt{r_{oN}^2 - r_{bN}^2} - r\cdot\sin(\phi) \qquad Z_{p1} = 0.231\ \text{in}$$

$$Z_{g1} := \sqrt{R_{oN}^2 - R_{bN}^2} - R\cdot\sin(\phi) \qquad Z_{g1} = 0.175\ \text{in}$$

$Z_N := Z_{p1} + Z_{g1}$ Length of Action in Mean Normal Section $Z_N = 0.406\ \text{in}$

$\Psi_b := \mathrm{acos}(\cos(\phi)\cdot\tan(\phi))$ Mean base spiral angle $\Psi_b = 70\ \text{deg}$

$$\eta := \sqrt{Z_N^2\cdot\cos(\Psi_b)^4 + F^2\cdot\sin(\Psi_b)^2} \qquad \eta = 0.449\ \text{in}$$

$f_I := \dfrac{Z_N}{2} - p_N$ Lowest Point of single tooth contact on the pinion (measurement from mid-point of the length of action) $f_I = -0.103\ \text{in}$

$$\eta_I := \sqrt{\eta^2 - 4\cdot f_I^2} \qquad \eta_I = 0.399\ \text{in}$$

$z_o := 0\text{in}$ $z_o = 0\ \text{in}$

$m_o := \dfrac{Z_N}{p_2}$ Transverse Contact Ratio $m_o = 0.155$

$$\rho_1 := \frac{r\cdot\sin(\phi)}{\cos(\Psi_b)^2} + z_o$$

$$\rho_2 := \frac{R\cdot\sin(\phi)}{\cos(\Psi_b)^2} - z_o$$

$\rho_o := \dfrac{\rho_1\cdot\rho_2}{\rho_1 + \rho_2}$ Relative Radius of Profile Curvature $\rho_o = 1.596\ \text{in}$

$C_i := 1$ Inertia Factor for I (use 1 for low pitch line speed)

$$\zeta_1(k_o) := \left[\eta_I^2 - 4\cdot k_o\cdot p_N\cdot(k_o\cdot p_N + 2\cdot f_I)\right]^3$$

$$\zeta_2(k_o) := \left[\eta_I^2 - 4\cdot k_o\cdot p_N\cdot(k_o\cdot p_N - 2\cdot f_I)\right]^3$$

$$\eta_{Ipcube} := \eta_I^3 + \sum_{ko=1}^{10}\left(\begin{cases}\sqrt{\zeta_1(ko)} & \text{if } \zeta_1(ko) > 0\\ 0 & \text{otherwise}\end{cases}\right) + \sum_{ko=1}^{10}\left(\begin{cases}\sqrt{\zeta_2(ko)} & \text{if } \zeta_2(ko) > 0\\ 0 & \text{otherwise}\end{cases}\right)$$

$m_{NI} := \dfrac{\eta_I^3}{\eta_{Ipcube}}$ Load Sharing Ratio $m_{NI} = 0.901$

$s_l := \dfrac{F\cdot Z_N\cdot\eta_I\cdot\cos(\Psi_b)}{\eta^2}$ Length of Line of Action $s_l = 0.131\ \text{in}$

$t_P := \frac{p}{2} - \frac{backlash}{2}$ Tooth Thickness, pinion $t_P = 0.194\ in$

$t_G := t_P$ Tooth Thickness, gear $t_G = 0.194\ in$

$b_P := b_g - .5 \cdot F \cdot \frac{b_g}{C}$ Mean Gear Dedendum $b_P = 0.124\ in$

$b_G := b_P$ Mean Pinion Dedendum $b_G = 0.124\ in$

$r_{fP} := \frac{(b_P - r_{TP})^2}{r + b_P - r_{TP}} + r_{TP}$ Fillet Radius at root of pinion tooth $r_{fP} = 0.052\ in$

$r_{fG} := \frac{(b_G - r_{TG})^2}{R + b_G - r_{TG}} + r_{TG}$ Fillet Radius at root of gear tooth $r_{fG} = 0.049\ in$

Formulae for Bending

$f_J := \frac{\eta}{2}$ Point of Load Application for Static Loading $f_J = 0.224\ in$

$\eta_J := \sqrt{\eta^2 - 4 \cdot f_J^2}$ $\eta_J = 0\ in$

$p_3 := \frac{Z_N}{2} + \frac{Z_N^2 \cdot f_J}{\eta^2}$ Point of load application for maximum bending stress. $p_3 = 0.387\ in$

$x_o := \frac{F \cdot \eta_J \cdot k \cdot Z_N}{\eta^2}$ $x_o = 0\ in$

$\phi_{LP} := \operatorname{atan}\left[\frac{p_3 + (r + R) \cdot \sin(\phi) - \sqrt{R_{oN}^2 - R_{bN}^2}}{r_{bN}}\right]$ $\phi_{LP} = 32.413\ deg$

$\phi_{LG} := \operatorname{atan}\left[\frac{p_3 + (r + R) \cdot \sin(\phi) - \sqrt{r_{oN}^2 - r_{bN}^2}}{R_{bN}}\right]$ $\phi_{LG} = 25.095\ deg$

Contact Stresses

$$C_p := \sqrt{\frac{1}{\pi\left(\frac{1-\nu_p^{\,2}}{E_p} + \frac{1-\nu_g^{\,2}}{E_g}\right)}}$$

Elastic coefficient $C_p = 2.268 \times 10^3 \sqrt{psi}$

$$C_s := \begin{cases} .125\cdot\frac{F}{in} + .4375 & \text{if } F > 0.5in \\ 0.5 & \text{otherwise} \end{cases}$$

Size Factor $C_s = 0.5$

$K_o := 1.0$

Overload Factor, taken as one because applied torque in this sheet is maximum torque

$K_v := 1.05$

See section 10 of AGMA 2003-B97

$$K_m := 1.1 + .0036\cdot\left(\frac{F}{in}\right)^2$$

Load distribution Factor for one member straddle mounted. This is only valid for crowned teeth.

$C_{xc} := 1.5$

Crowning factor (for properly crowned teeth)

Determination of the Geometry Factor For Durability

$$I := \frac{s_l\cdot\rho_o\cdot\cos(\phi)}{F\cdot D_p\cdot C_i\cdot m_{NI}}\cdot\frac{P_d}{P_m}$$

Result $I = 0.234$

Contact Stress Result

$$S_c := C_p\cdot\sqrt{\frac{2\cdot T_p}{F\cdot D_p^{\,2}\cdot I}\cdot K_o\cdot K_v\cdot K_m\cdot C_s\cdot C_{xc}}$$

$S_c = 2.458 \times 10^5\,psi$ Contact Stress Number

Related Gear Formulae

$$\theta_{hP} := .5\cdot\frac{t_P}{r} - \left(\tan\left(\phi_{LP}\right) - \phi_{LP}\right) + \left(\tan(\phi) - \phi\right)$$

$\theta_{hP} = 3.59\,deg$

$$\theta_{hG} := \frac{.5\cdot t_G}{R} - \left(\tan\left(\phi_{LG}\right) - \phi_{LG}\right) + \left(\tan(\phi) - \phi\right)$$

$\theta_{hG} = 2.612\,deg$

$\phi_{hP} := \phi_{LP} - \theta_{hP}$ $\phi_{hG} := \phi_{LG} - \theta_{hG}$

$$\Delta r_N := \frac{r_{bN}}{\cos\left(\phi_{hP}\right)} - r \qquad \Delta R_N := \frac{R_{bN}}{\cos\left(\phi_{hG}\right)} - R$$

$r_t := r \cdot \left(\frac{C_m + x_o}{C_m} \right) + \Delta r_N$ Mean Transverse Radius of Pinion to Load Application $r_t = 0.891 \text{ in}$

$R_t := R \cdot \left(\frac{C_m + x_o}{C_m} \right) + \Delta R_N$ Same, for gear $R_t = 1.62 \text{ in}$

$y_{2P} := b_P - r_{TP}$

$x_{oP} := .5 \cdot t_P + b_P \cdot \tan(\phi) + r_{TP} \cdot (\sec(\phi) - \tan(\phi))$

$X_{\theta P} := x_{oP} + y_{2P}$

Use MATHCAD to solve for XθP. The equasions below are combined into one very large equasion in the following line.

Given

$$\frac{\left[r \cdot \sin\left(\frac{X_{\theta P}}{r}\right) - r_{TP} \cdot \cos\left[\operatorname{atan}\left[\frac{y_{2P} \cdot \cos\left(\frac{X_{\theta P}}{r}\right) - (X_{\theta P} - x_{oP}) \cdot \sin\left(\frac{X_{\theta P}}{r}\right)}{y_{2P} \cdot \sin\left(\frac{X_{\theta P}}{r}\right) + (X_{\theta P} - x_{oP}) \cdot \cos\left(\frac{X_{\theta P}}{r}\right)} \right] \right] - \left[y_{2P} \cdot \sin\left(\frac{X_{\theta P}}{r}\right) + (X_{\theta P} \right.}{\Delta r_N + r \cdot \left(1 - \cos\left(\frac{X_{\theta P}}{r}\right)\right) + r_{TP} \cdot \sin\left[\operatorname{atan}\left[\frac{y_{2P} \cdot \cos\left(\frac{X_{\theta P}}{r}\right) - (X_{\theta P} - x_{oP}) \cdot \sin\left(\frac{X_{\theta P}}{r}\right)}{y_{2P} \cdot \sin\left(\frac{X_{\theta P}}{r}\right) + (X_{\theta P} - x_{oP}) \cdot \cos\left(\frac{X_{\theta P}}{r}\right)} \right. \right.}$$

$X_{\theta P} := \text{Minerr}(X_{\theta P})$ $X_{\theta P} = 0.183 \text{ in}$

$\theta_P := \frac{X_{\theta P}}{r}$

$x_{2P} := X_{\theta P} - x_{oP}$

$z_{1P} := y_{2P} \cdot \cos(\theta_P) - x_{2P} \cdot \sin(\theta_P)$

$z_{2P} := y_{2P} \cdot \sin(\theta_P) + x_{2P} \cdot \cos(\theta_P)$

$\zeta_P := \operatorname{atan}\left(\frac{z_{1P}}{z_{2P}}\right)$

$t_{NP} := r \cdot \sin(\theta_P) - r_{TP} \cdot \cos(\zeta_P) - z_{2P}$ $t_{NP} = 0.141 \text{ in}$

$h_{NP} := \Delta r_N + r \cdot (1 - \cos(\theta_P)) + r_{TP} \cdot \sin(\zeta_P) + z_{1P}$ $h_{NP} = 0.198 \text{ in}$

$X_{NP} := \frac{t_{NP}^{\,2}}{h_{NP}}$ Pinion Tooth Strength Factor $X_{NP} = 0.1 \text{ in}$

$$Y_P := \frac{2}{3}\cdot\frac{P_d}{\frac{1}{X_{NP}} - \frac{\tan(\phi_{hP})}{3\cdot t_{NP}}}$$ Pinion Tooth Form Factor $Y_P = 0.611$

$y_{2G} := b_G - r_{TG}$

$x_{oG} := .5\cdot t_G + b_G\cdot\tan(\phi) + r_{TG}\cdot(\sec(\phi) - \tan(\phi))$

$X_{\theta G} := x_{oG} + y_{2G}$

Given

$$\frac{\left[R\cdot\sin\left(\frac{X_{\theta G}}{R}\right) - r_{TG}\cdot\cos\left[\operatorname{atan}\left[\frac{y_{2G}\cdot\cos\left(\frac{X_{\theta G}}{R}\right) - (X_{\theta G} - x_{oG})\cdot\sin\left(\frac{X_{\theta G}}{R}\right)}{y_{2G}\cdot\sin\left(\frac{X_{\theta G}}{R}\right) + (X_{\theta G} - x_{oG})\cdot\cos\left(\frac{X_{\theta G}}{R}\right)}\right]\right]\right] - \left[y_{2G}\cdot\sin\left(\frac{X_{\theta G}}{R}\right) + (X_{\theta}\right.}{\Delta R_N + R\cdot\left(1 - \cos\left(\frac{X_{\theta G}}{R}\right)\right) + r_{TG}\cdot\sin\left[\operatorname{atan}\left[\frac{y_{2G}\cdot\cos\left(\frac{X_{\theta G}}{R}\right) - (X_{\theta G} - x_{oG})\cdot\sin\left(\frac{X_{\theta G}}{R}\right.}{y_{2G}\cdot\sin\left(\frac{X_{\theta G}}{R}\right) + (X_{\theta G} - x_{oG})\cdot\cos\left(\frac{X_{\theta G}}{R}\right.}\right.\right.}$$

$X_{\theta G} := \operatorname{Minerr}(X_{\theta G})$ $X_{\theta G} = 0.199\ in$

$$\theta_G := \frac{X_{\theta G}}{R}$$

$x_{2G} := X_{\theta G} - x_{oG}$

$z_{1G} := y_{2G}\cdot\cos(\theta_G) - x_{2G}\cdot\sin(\theta_G)$

$z_{2G} := y_{2G}\cdot\sin(\theta_G) + x_{2G}\cdot\cos(\theta_G)$

$$\zeta_G := \operatorname{atan}\left(\frac{z_{1G}}{z_{2G}}\right)$$

$t_{NG} := R\cdot\sin(\theta_G) - r_{TG}\cdot\cos(\zeta_G) - z_{2G}$ $t_{NG} = 0.145\ in$

$h_{NG} := \Delta R_N + R\cdot(1 - \cos(\theta_G)) + r_{TG}\cdot\sin(\zeta_G) + z_{1G}$ $h_{NG} = 0.156\ in$

$$X_{NG} := \frac{t_{NG}^2}{h_{NG}}$$ Gear Tooth Strength Factor $X_{NG} = 0.134\ in$

$$Y_G := \frac{2}{3}\frac{P_d}{\frac{1}{X_{NG}} - \frac{\tan(\phi_{hG})}{3 \cdot t_{NG}}}$$ Gear Tooth Form Factor $Y_G = 0.822$

Stress Concentration Factor

$$H := .3254545 - .0072727 \cdot (\phi \cdot 57.3)$$

$$L := .3318182 - .0090909 \cdot (\phi \cdot 57.3)$$

$$M := .2681818 + .0090909 \cdot (\phi \cdot 57.3)$$

$$K_{fP} := H + \left(\frac{2 \cdot t_{NP}}{r_{fP}}\right)^L \cdot \left(\frac{2t_{NP}}{h_{NP}}\right)^M$$ $K_{fP} = 1.687$

$$K_{fG} := H + \left(\frac{2 \cdot t_{NG}}{r_{fG}}\right)^L \cdot \left(\frac{2 \cdot t_{NG}}{h_{NG}}\right)^M$$ $K_{fG} = 1.906$

Tooth Form Factor

$$Y_{KP} := \frac{Y_P}{K_{fP}}$$ $Y_{KP} = 0.362$

$$Y_{KG} := \frac{Y_P}{K_{fG}}$$ $Y_{KG} = 0.32$

$m_N := 1.0$ Tooth Load Sharing Factor, use 1 for statically loaded gears

$$F_K := \frac{F \cdot Z_N \cdot \eta_J \cdot \cos(\Psi_b)^2}{\eta^2}$$ Projected length of the instantaneous line of contact in the lengthwise direction of the tooth $F_K = 0\ \mathrm{in}$

Effective Pinion Facewidth

$$\Delta F_{TP} := \frac{F_P - F_K}{2} + x_o$$ $\Delta F_{TP} = 0.238\ \mathrm{in}$

$$\Delta F_{HP} := \frac{F_P - F_K}{2} - x_o$$ $\Delta F_{HP} = 0.238\ \mathrm{in}$

$$F_{eP} := h_{NP} \cdot \left(\mathrm{atan}\left(\frac{\Delta F_{TP}}{h_{NP}}\right) + \mathrm{atan}\left(\frac{\Delta F_{HP}}{h_{NP}}\right)\right) + F_K$$ $F_{eP} = 0.347\ \mathrm{in}$

Effective Gear Facewidth

$$\Delta F_{TG} := \frac{F_G - F_K}{2} + x_o$$

$$\Delta F_{HG} := \frac{F_G - F_K}{2} - x_o$$

$$F_{eG} := h_{NG} \cdot \left(\operatorname{atan}\left(\frac{\Delta F_{TG}}{h_{NG}} \right) + \operatorname{atan}\left(\frac{\Delta F_{HG}}{h_{NG}} \right) \right) + F_K \qquad F_{eG} = 0.309\ in$$

Bending Stress: Pinion

$K_s := .4867 + \dfrac{.2133}{P_d \cdot in}$ Size factor for bending

$K_x := 1.0$ Lengthwise curvature factor (1.0 for strait bevel)

Determination of the Geometry Factor for Bending

$$J_p := \frac{Y_{KP}}{m_N \cdot C_i} \cdot \frac{r_t}{r} \cdot \frac{F_{eP}}{F} \cdot \frac{P_d}{P_m} \qquad J_p = 0.235$$

Bending Stress Result

$$S_{tp} := \frac{2 \cdot T_p}{F \cdot D_p} \cdot P_d \cdot K_o \cdot K_v \cdot K_s \cdot \frac{K_m}{K_x \cdot J_p}$$

$S_{tp} = 1.039 \times 10^5\ psi$ Pinion Bending Stress Number

Bending Stress: Gear

Determination of the Geometry Factor for Bending

$$J_g := \frac{Y_{KG}}{m_N \cdot C_i} \cdot \frac{R_t}{R} \cdot \frac{F_{eG}}{F} \cdot \frac{P_d}{P_m} \qquad J_g = 0.176$$

Bending Stress Result

$$S_{tg} := \frac{2 \cdot T_g}{F \cdot D_g} \cdot \frac{P_d \cdot K_o \cdot K_v \cdot K_s \cdot K_m}{K_x \cdot J_g}$$

$S_{tg} = 1.391 \times 10^5\ psi$ Gear Bending Stress Number

Reaction Forces

Side Gear

$$F_t := \frac{\dfrac{T_{app}}{2 \cdot N_p}}{C_m \cdot \sin(\Gamma_g)} \qquad F_t = 2.949 \times 10^3\,\text{lbf}$$

$$F_r := F_t \cdot \tan(\phi) \cdot \cos(\Gamma_g) \cdot N_p \qquad F_r = 1.257 \times 10^3\,\text{lbf}$$

$$F_a := F_t \cdot \tan(\phi) \cdot \sin(\Gamma_g) \cdot N_p \qquad F_a = 1.74 \times 10^3\,\text{lbf}$$

Spyder Gear

$$F_r := F_t \cdot \tan(\phi) \cdot \sin(\Gamma_g) \cdot 2 \qquad F_r = 1.74 \times 10^3\,\text{lbf}$$

$$F_a := F_t \cdot \tan(\phi) \cdot \cos(\Gamma_g) \cdot 2 \qquad F_a = 1.257 \times 10^3\,\text{lbf}$$

Material Properties

Allowable Contact Stress

$$s_{ac} := 250 \cdot 10^3\,\text{psi}$$

$$N_L := 20000 \cdot 140 \cdot N_p \cdot \frac{Z_g}{Z_p}$$ Required Number of loading cycles $N_L = 7.754 \times 10^6$

$$C_L := 3.4822 \cdot N_L^{-.0602}$$ Fatigue Factor $C_L = 1.34$

$$B_1 := .00898 \cdot \left(\frac{HRC\_TO\_HBN(H_p)}{HRC\_TO\_HBN(H_g)} \right) - .00829$$

$$C_H := 1 + B_1 \cdot \left(\frac{Z_g}{Z_p} - 1 \right)$$ Hardness Ratio Factor $C_H = 1$

$K_T := 1.0$ Temperature Factor (I don't expect the diff to get above 250 F)

$C_r := 1.12$ Reliability factor (1.12 for 1 failure in 1000)

$S_F := 1.0$ Safety Factor

$$s_{wc} := \frac{s_{ac} \cdot C_L \cdot C_H}{S_F \cdot K_T \cdot C_r}$$ Allowable Contact Stress $s_{wc} = 2.992 \times 10^5\,\text{psi}$

Allowable Bending Stress

$$s_{at} := 40 \cdot 10^3\,\text{psi}$$

$K_R := 1.25$ Reliability Factor (1.25 for 1 failure in 1000)

$$K_L := \begin{cases} 6.1514 \cdot \left(N_L^{-.1192}\right) & \text{if } N_L < 2 \cdot 10^6 \\ 1.683 \cdot \left(N_L^{-.0323}\right) & \text{otherwise} \end{cases}$$

$K_L = 1.008$

$K_{rev} := 0.70$ For Fully Reversed Loading

$s_{wt} := s_{at} \cdot \dfrac{K_L \cdot K_{rev}}{S_F \cdot K_T \cdot K_R}$ Allowable Bending Stress Number $s_{wt} = 2.258 \times 10^4 \, psi$

$S_{tg} = 1.391 \times 10^5 \, psi$

$s_{wt} = 2.258 \times 10^4 \, psi$

$S_{tp} = 1.039 \times 10^5 \, psi$

$S_c = 2.458 \times 10^5 \, psi$ $s_{wc} = 2.992 \times 10^5 \, psi$

$SF_{tg} := \dfrac{s_{wt}}{S_{tg}}$ $SF_{tg} = 0.162$

$SF_{tp} := \dfrac{s_{wt}}{S_{tp}}$ $SF_{tp} = 0.217$

$SF_c := \dfrac{s_{wc}}{S_c}$ $SF_c = 1.217$